UNIVERSITY OF
KWAZULU-NATAL

INVESTIGATION OF THE STRUCTURAL RESPONSE

OF

THE GROOT OLIFANTS RIVER BRIDGE TO SEISMIC EXCITATION

By

Jan Mabeke Phakwago

Student No: 213569847

Submitted in fulfilment of the academic requirements for the degree of
Master of Science in Engineering - Civil

School of Civil Engineering, Surveying and Construction
University of KwaZulu-Natal
Durban
November 2019

ABSTRACT

The South African freight railway owner (Transnet fright rail) has over 5000 bridges servicing its railway network. Majority of those bridges are deemed to have exceeded their proposed design lives and cannot support the increasing traffic loads which are significantly greater than the loads they were designed to carry. Moreover, most of those bridges were not designed for seismic excitation as the South African codes of practice at the time did not take seismic action into consideration. This study investigates the structural behaviour of the 32m span Groot Olifants river bridge to seismic excitation. The investigation focuses on the bridge superstructure. Numerical modelling of the Groot Olifants river bridge was carried out in order to simulate the experimental test performed in the field. Digital image correlation (DIC) techniques were used to take field measurements of the deformations on the bridge. The computational programme, ANSYS, was used to perform a finite element analysis in order to assess the structural response of the bridge. The deflection measurements obtained from the DIC were used to validate the accuracy of the FEA model. The ultimate load capacity of the main truss elements in the bridge was determined and compared to the response from the numerical analysis in order to evaluate the potential failure of the bridge when subjected to seismic excitation. The study incorporates field load tests, finite element analysis as well as a case study of a similar bridge tested to ultimate load failure in Sweden. The results indicate that the bridge can resist low intensity seismic events when evaluated using the response spectrum analysis. However, from the transient structural analysis it is concluded that the Groot Olifants river bridge is susceptible to the high intensity seismic event predicated by Visser and Kijko (2010). From the field tests, it is further concluded that the Groot Olifants river bridge can resist the heavier loads to be applied by the new 44D locomotives.

Education is key. This thesis is a result of sleepless nights, ample frustration and unwillingness to quit. Education aluta continua.

DECLEARATION

Supervisor:

As the candidate's supervisor, I agree to the submission of this dissertation.

Signed: …. ………... **Dr. Georgios A. Drosopoulos** Date: 9/8/2020 ……………………

Candidate:

I, Jan Mabeke Phakwago, declare that;

1) The work presented in this dissertation was carried out at the University of Kwazulu Natal (Durban) in the college of Agriculture, Engineering and Science.

2) This dissertation is the results of my own work and any quotation from, or description of the work of others is acknowledged herein by reference to the sources.

3) The work contained herein has not been submitted in part, or in whole to this or any other University for another qualification.

4) This dissertation does not contain other persons' writing, unless specifically acknowledged as being sourced from other researchers. Where other written sources have been quoted, then:

   a. Their words have been re-written, but the general information attributed to them has been referenced

   b. Where their exact words have been used, then their writing has been placed in inside quotation marks and referenced,

   c. This dissertation does not contain text, graphics or tables copied and pasted from the Internet, unless specifically acknowledged, and the source being detailed in the thesis and in the References sections.

Signed by: **JAN MABEKE PHAKWAGO,** student No: **213569847** at **University of**

Kwazulu Natal. Date: **9 November 2019** Signature: …………….…..

Supervisor

Dr. G.A Drosopoulos

College of Agriculture, Engineering and Science

University of Kwazulu Natal

(Howard college campus)

Durban

Page intentionally left blank

Acknowledgements

Praise and thanks be to God almighty for his showers of blessings throughout my studies.

I would like to thank my family for the support and encouragement that they provided throughout my studies. The endless love and motivation form all my siblings have been invaluable.

I would like to express my sincere gratitude to my supervisor Dr. G.A Drosopoulos for the assistance and guidance he provided enabling me to complete this dissertation. This dissertation would not have been possible without your guidance and willing presence as well as the valuable expertise and insight in the field of structural Engineering & computational mechanics. I greatly appreciate the patience you had to allow me to explore the various angles to this research.

Table of contents

List of Figures

List of Tables

CHAPTER 1

1.1 Introduction

There are over 5000 bridges servicing the South African state-owned freight rail company (Transnet), which generates revenue of over 25 billion Rands per annum (Molefe; 2018). Majority of these railway bridges are old and have reached the end of their proposed design life. As a result, they cannot support the increasing traffic loads which are significantly greater than the loads the bridges were designed to carry. In addition, most of these old bridges were not designed for seismic excitation as civil engineering professionals at the time, were not required to design bridges to resist earthquake loads prior to 1981 (Solms, 2016). The Groot Olifants river bridge is one of the railway bridges that forms a major infrastructural investment for the South African government. It is located on the eastern railway line between Witbank and Middelburg in Mpumalanga province (South Africa). Transnet freight rail is currently undertaking an intensive research on the bridge, to determine the feasibility of increasing the axle load in order to increase revenue generated from the eastern region.

Research by Moyo & Busatta (2015) has revealed that new and emerging mines in South Africa, as well as strong competition among coal exporting to other countries has led to a progressive increase in the capacity of the railway line. This was achieved by using a combination of operating strategies which included, increasing the axle load of wagons, increasing the train speed as well as increasing the length of trains (Kuys, 2009). As a result, the South Africa freight railway owner (Transnet freight rail) has over the years, invested significantly in the investigation of new and efficient technologies in telecommunication and signalling systems (Von Gericke, 1986), track superstructure, as well as rolling stock technology (Veldsman & Mulde, 2005). Moreover, Moyo and Busatta (2015) contend that maintenance strategies have also been improved in order to sustain the increased rail capacity demands and limit the negative effects (rail degradation, track instability etc.) occurring when heavier and/or longer trains are hauled. Conversely, the structural response of South African railway bridges to seismic excitation has been neglected The south African railway owner has advanced minor efforts to investigate the structural behaviour of railway bridges subjected to earthquake loading, yet any damage or collapse of railway bridge infrastructure resulting from earthquake action would cause serious disruption to traffic flow, reduce capacity, have severe impacts on the economy of South Africa and result in significant loss of Human life. Moreover, the lack of funding as well as the extensive time required to replace aging railway bridges necessitates the present investigation.

This dissertation will not attempt to develop a new method of analysis for bridges subjected to seismic loads but will instead use currently available commercial software to investigate the structural response of the Groot Olifants steel bridge to seismic excitation. The Groot Olifants river bridge was designed for a load carrying capacity of 22 tonnes/axle (220KN/axle). Investigation focusing on the feasibility of increasing the ultimate load capacity of the Groot Olifants river bridge is currently underway. To this extend, static and dynamic load tests were conducted on the Olifants river bridge. This study incorporates static field tests, a case study of a structurally similar bridge, as well as finite element analysis. The field test results were used to validate the accuracy of the numerical models employed to assess the structural behaviour of the bridge when subjected to earthquake loading as specified in the South African bridge code and TMH7.

1.2 Research problem.

South Africa has a considerable amount of steel railway bridges which are maintained by Transnet freight rail depots in the respective regions. Majority of these bridges were designed and constructed using codes that did not take seismic action into account because South Africa was not considered to be an earthquake prone region like Japan or India. However, in recent years, South Africa experienced moderate seismic activities that resulted in serious damage to infrastructure, such as buckled and collapsed piers, cracks in concrete structures (Abutments) as well as the loss of life. In 2014, the South African local Council for Geoscience (CGS) recorded two earthquakes in the Northwest province, with Richter scale magnitudes of 5.5 and 4.9 respectively, (Visser & Kijko, 2010). This indicates that while seismic events are comparatively rare in South Africa, they can still occur from time to time. In regions with structures unprepared for seismic activity (like in South Africa), it has been proven that slight earth movement can produce hundreds of thousands of casualties (Visser & Kijko, 2010).

From the above observation, the need for a comprehensive investigation into the structural response of steel bridges to seismic action is identified. Such investigation will help bridge authorities and design consultants to have a clear understanding of the structural response of steel bridges to seismic action in order improve design practices and ensure public safety.

1.3 Aims and objectives

The aims of this study are as follows;

- ➢ To investigate the structural response of steel bridges to seismic excitation, considering mainly deflections and structural behaviour

- ➢ To investigate the feasibility of running heavier trains (44D locomotives) on old steel bridges designed for lower train loads.

The objective of the study is;

- ➢ To better understand the load-carrying mechanism, gain insight into the ultimate load-carrying capacity of existing bridges and study the structural response of bridges during earthquakes.

1.4 Limitations

Due to time constraints and computational limitations, the dissertation has been limited to the analysis of the bridge superstructure only.

1.5 Layout of dissertation

This dissertation is divided into five chapters as follows:

Chapter 1:

Chapter 1 provides an introductory background to the topic, focusing mainly on the basis for the research. It then provides the layout of the dissertation as well as the aims and objectives.

Chapter 2

Chapter 2 provides a literature review on seismic design. The chapter first gives a brief historical background on the seismicity of South Africa. It then examines the current South African bridge design code, considering mainly the different methods of analysis, selection of design spectrum and earthquake category

Chapter 3

In chapter 3, the methodology used to study the structural response of the Groot Olifants river bridge to seismic excitation is presented. The chapter first provides a detailed description of the bridge as well as field tests performed. The commercial software (ANSYS) is then used to investigate the structural response of the bridge. The chapter

ends by providing a brief case study of the work carried out by the Luleå University of Technology on the Åby river bridge in order to compare and validate the behaviour observed from the FEA carried out on the Groot Olifants river bridge.

Chapter 4

In chapter 4, the results obtained from the analysis carried out in chapter 3 are presented and discussed. Firstly, a comparison of the numerical results with the field measurements is provided. The tabulated results and graphical solutions are then analysed and interpreted.

Chapter 5

Chapter 5 provides the conclusions reached in this investigation. The chapter then provide recommendations for future studies.

CHAPTER 2

Literature review

2.1 Seismic risk of the region

The seismicity of Africa (especially Southern Africa) is by world standards, very moderate and of shallow character (Brandt, 2011). However, seismic excitation poses a catastrophic hazard to all bridge structures situated in non-earthquake prone zones (Banerjee & Ganesh, 2013). Over the years, numerous bridges sustained serious damage, while others completely collapsed due to the seismic action in regions which were previously deemed to be non-earthquake prone zones (Yanev et al., 2010, Soetardjo et el., 1985, Toshiro et el., 2000). According to Solms (2016), 'The occurrence of moderate intensity earthquakes is uncommon in South Africa, with only a limited number of moderate to strong seismic events occurring in the past'. Table 2.1 provides a list of significant seismic activities recorded in South Africa. (Kijko, Durrheim & Mayshree, 2009)

Table 2.1; Major recorded seismic events that occurred in South Africa (After Durrheim et al.,2009)

Date	Magnitude (Richter)	Location	Damage
1809	6.3	Cape town region	Collapse of farmhouses
1932	6.3	Cape St Lucia	Extensive damage to buildings. Cracks in road surfaces and bridges.
1969	6.3	Tulbagh	Loss of life. Extensive damage to buildings including total collapse. Cracks in road surfaces and bridges.
1976	5.2	Welkom	Extensive damage to buildings including total collapse.
1991	5.0	Ceres	Extensive damage to buildings.

Research by Brandt & Saunders (2011) proved that certain regions of South Africa are prone to moderate intensity earthquakes. Visser and Kijko (2010) predict that an earthquake with an estimated magnitude ranging between 6.0 and 6.87 and a return period of approximately 475 years could be expected in South Africa. An earthquake with a magnitude of 6.87 would result in level IX shaking intensity on the Mercalli Magnitude Intensity (MMI) scale (Visser & Kijko, 2010). This would result in severe damage to the infrastructure as well as loss of life. According to Haas & Kolf (2014), Visser & Kijko (2010), countries that have ineffective seismic provisions in their design codes of practice, as well as those that do not incorporate seismic loading in the design of their infrastructure are at risk of sustaining major damage and even complete collapse of their civil engineering infrastructure. Consequently, it is important for countries that are at risk of moderate to severe seismic action (like South Africa) to incorporate a robust seismic loading code of practice to ensure that its civil engineering infrastructure can resist the effect of seismic excitation.

2.2 Seismic induced failure in bridges.

Bridge supports, abutments, piers, bearings as well as bridge decks are the most vulnerable parts of a bridge during an earthquake. Seismic action during an earthquake causes vertical and horizontal ground motions that can lead to structural failure of bridges. Those vertical and horizontal ground motions may cause soil liquefaction at the foundation, reducing the load-carrying capacity of the bridge, leading to failure (Wang et al., 2013, Hashimoto & Chouw, 2003). The most common form of bridge substructure failure resulting from seismic action includes failure from fluctuating axial forces, shear-flexural failure of the bridge pier as well as local buckling of piers (Yang & Lee, 2007, Wang et al., 2013). In the bridge superstructure, the most common form of failure observed from historic analysis of bridges subjected to seismic action is attributed to transverse and longitudinal movement of the bridge superstructure. The ground motion generates internal forces ($F_{Inertial}$ equ (1)) in the structural components, resulting in structural damage.

$$F_{Inertial} = m \times a \qquad (1)$$

Where; m = Mass

a = Acceleration.

2.3 Bridge Substructure failure modes.

Research indicates that bridge piers subjected to seismic action are more likely to fail in one of three modes, namely, shear failure (Priestley et el., 1994), flexural failure (Hwang et al., 2000) and crushing failure (Kim et al., 2011). During an earthquake, the vertical ground motion causes substantial fluctuating axial forces in the bridge piers, resulting in outward buckling or crushing of the piers as indicated in figures 2.1 -2.3 (Kunnath et al., 2008, Kim et al., 2011). The horizontal ground motion significantly amplifies the shear force in the bridge substructure, leading to the failure of bridge piers (Sun et al., 2012). According to Kim et al (2011), most damage to reinforced concrete piers can be attributed to inadequate detailing of reinforcement, which limits the ability of the column to deform inelastically. Therefore, the inadequate detailing of reinforced concrete piers causes the piers to experience large inelastic demands resulting in the formation of local buckling accompanied by visible plastic deformation. The local buckling is often the primary cause of bridge collapse.

Figure 2.1; Failure of column with longitudinal reinforcement cut-off near mid-height in 1995 Hyogo -Ken Nanbu earthquake (Chen and Duan: 1999)

3

Figure 2.2;Local Buckling of a circular cross section column of the Hanshin expressway in 1995 hyogo Ken Nanbu earthquake, (Chen and Duan: 1999)

Figure 2.3; Collapse of a rectangular cross section steel column in the 1995 Hygo - Ken Nanbu earthquake. (a) collapsed bent superstructure;(b) close-up collapsed column (Chen and Duan: 1999)

2.4 Bridge superstructure failure

The study of historic bridge failure due to seismic action has indicated that failure of the bridge superstructure is generally a secondary effect and does not cause the total collapse of the bridge. The horizontal ground motion causes the beams and girder to slide in the transverse or longitudinal direction due to weak connections between the bridge superstructure and substructure (Saadeghvaziri & Yazdani-Motlagh, 2008). This sliding movement can lead to impact between the end-span and the abutment, as well as ponding between adjacent spans in multi-span bridges (figure 2.4). The sliding impact between the bridge superstructure and substructure can result in the shear failure of the bridge bearings (Nielson & DesRoches 2006, Pan et al., 2010), the bridge girder (figure 2.5) as well as the failure of abutment backwalls (DesRoches et al., 2004, Saadeghvaziri & Yazdani-Motlagh 2008). The movement of the bridge superstructure further causes the failure of the bridge bracing system (figure 2.5) which significantly reduces the stability in bridges.

Figure 2.4; Santa Clara river bridge ponding damage in 1994 Northridge earthquake. (a) Barrier rail pounding damage; (b) abutment damage (Chen and Duan: 1999)

Figure 2.5; Buckling of the cross members in the upper chord of the Rokko island bridge in the Hyogo Nanbu earthquake (Chen and Duan: 1999)

Figure 2.6; Damage to girder of the bridge on the Hanshin express way due to the transverse movement in the 1995 Hyogo Nanbu earthquake (Chen and Duan:1999)

2.5 Impacts of bridge failure

Earthquakes cause damage to all structures, including bridges. Major earthquakes can bring about the collapse of dozens of buildings, but collapsed bridges are often the most visible signs of the impacts an earthquake can have. In recent years, the tragic collapse of the Morandi bridge in Genoa Italy (August 2018) illustrated the devastating impacts of bridge collapse. The collapse of the Morandi bridge was not due to seismic action, however, it caused massive traffic problems, injury, loss of life and had severe economic consequences, (Genoa news: 2018).

Figure 2.7; Impacts of Morandi Bridge collapse (Genoa news:2018).

In 1989, Loma Prieta earthquake stroke the California coastal cities of Oakland and San Francisco, causing 63 deaths (Yashinsky, 1998). Majority of the deaths occurred as a result of two bridges that collapsed. The collapse of the bridges created immediate damage to vehicles that were on the structure at the time, damage to rail cars below the bridge, and disturbance to the ground below the bridge. Bridge debris and construction materials being stored on the bridge deck were also deposited into the river flowing below the bridge, causing flow and possible habitat disruption, and potential contamination risks. During a bridge collapse, the bridge materials become potential sources of hazardous air, water, and soil contamination.

2.6 South African design code

The present South African Code of Practice for the design of Highway Bridges and Culverts (TMH 7- parts 1-3) was adopted in 1983 and has not been modified since then. THM 7 contains the requirements for the seismic design of bridges in South Africa. These include provisions regarding seismic loading, design spectra, methods of analysis, as well as earthquake category. The code aims to improve the structural behaviour of bridges in order to enable them to withstand seismic effects, preventing collapse during major earthquakes. However, the South African seismic loading conditions as stipulated in the industrial structures and buildings loading code (SANS 10160-4) as well as the bridge code (in TMH7) are considered to be too stringent and result in uneconomic designs (Wium, 2010). In South Africa, railway bridges are designed in accordance with THM7 (part 1-3) in conjunction with the South African transport services bridge code of 1983 (SATS, 1983).

2.6.1 Earthquake Category

TMH7 (1983) defines South African seismic regions on a seismic intensity map (Figure 2.8). The map is based on the distribution of expected intensity levels expressed in terms of the MMI scale and classified in terms of peak ground accelerations (PGA) Table 2.3. According to the seismic intensity map (figure 2.8), the Groot Olifants river bridge was supposed to have been designed for a MMI level VI earthquake, which corresponds to a design ground acceleration of 0.1g. The seismic intensity map found in THM7 (though relevant) is old and outdated. This indicates the need for a revision to TMH7.
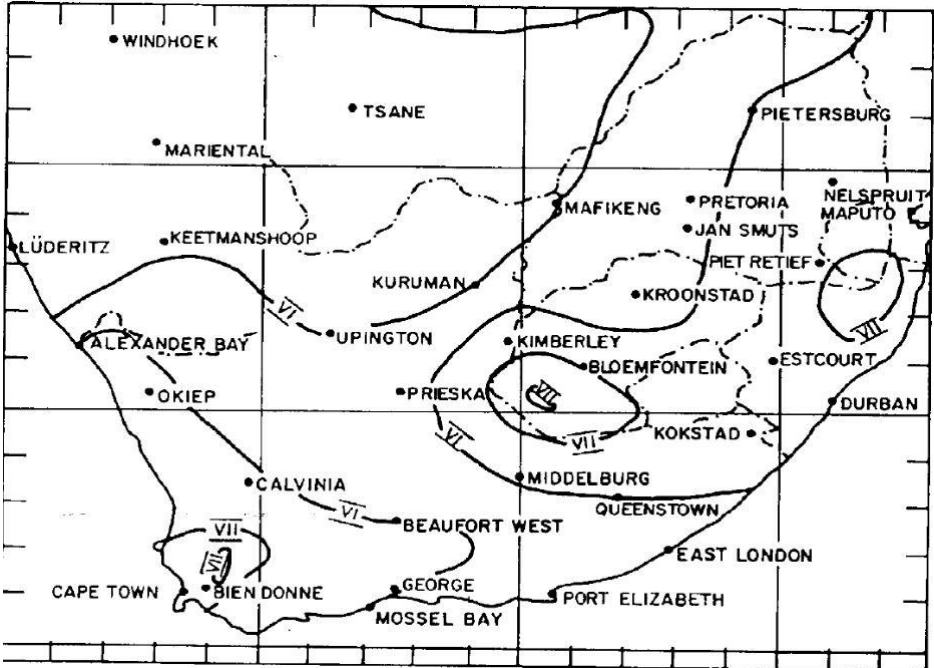
Figure 2.8; Seismic intensity map (TMH7: 1983)

Table 2.2; Modified Mercalli classification (TMH7;1983)

Modified Mercalli Intensity at epicenter (MMI)	Maximum ground acceleration (a) at epicenter
ii – iii	0.003g
iv – v	0.01g
vi	0.03g
vii – viii	0.1g
ix	0.3g
x – xi	1.0g

2.6.2 Design spectra

The TMH7 design code provides the peak ground motion bounds and the average response spectrum which is normalized to a ground acceleration of 1.0 g. The deformation, pseudo-velocity, and pseudo-acceleration design spectra for the given ground motion are illustrated in figure 2.9. The deformation, pseudo-velocity, and pseudo-acceleration design spectrum are different ways of presenting the same information on structural response. The deformation spectrum is useful in that it provides the peak deformation of a system, while the pseudo-velocity spectrum provides information relating to the strain energy stored in the system as a result of seismic action. The pseudo-acceleration spectrum is used to determine the equivalent static force and base shear in the structure. The design spectrum is based on statistical analysis of the response spectra for the ensemble of ground motions (Chopra, 1978). The selection of the design spectrum depends on many parameters such as the site category, damping ratio of structure and soil properties. TMH7(1983) has provision for modifying the design response spectrum for bridges to undergo elastic-plastic deformation when subjected to seismic action. According to the TMH7(1983), for a given damping ratio, the elastic design spectrum is modified along the displacement and acceleration bounds region. For this modification, the elastic spectrum (displacement bound line) is multiplied by the ductility factor ($\frac{1}{\mu}$) to get the inelastic spectrum used for design, while the acceleration bound line is multiplied by a factor of $\frac{1}{\sqrt{2\mu-1}}$

Where μ is the ductility factor $= \dfrac{total\ elastic-plactic\ deformation}{total\ elastic\ deformation\ at\ yield}$

Figure 2.9 provides a graphic presentation of the transformation from elastic to elastic - plastic design spectrum.
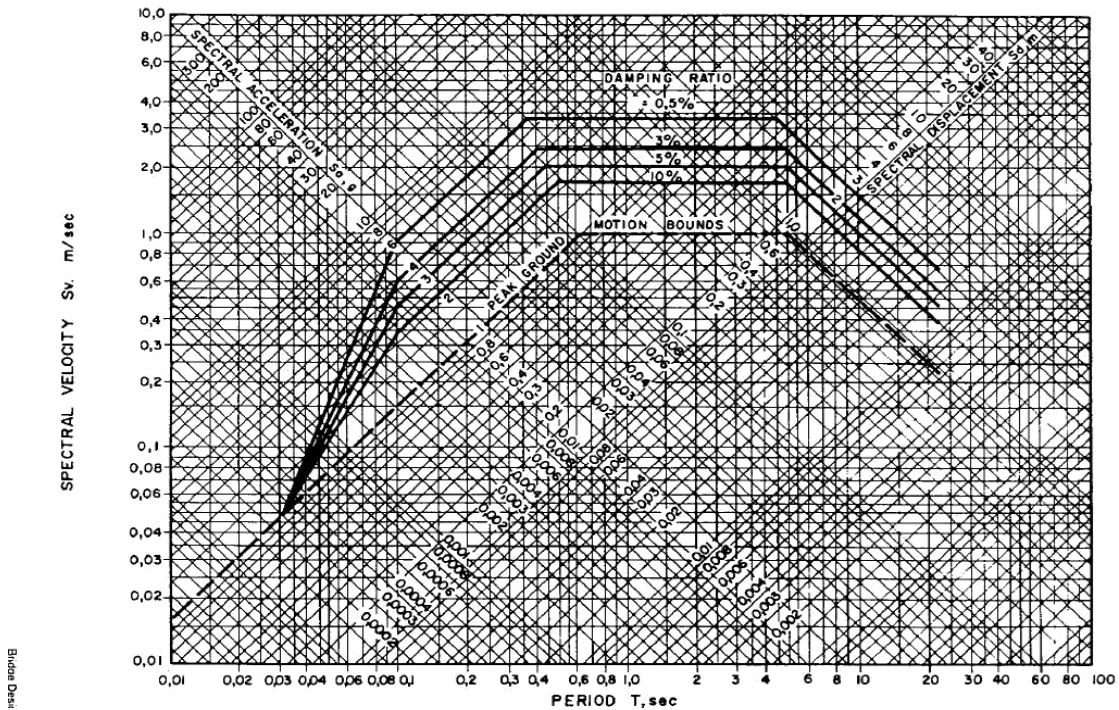
Figure 2.9; Peak ground motion bounds and average elastic response spectrum (TMH7; 1983).
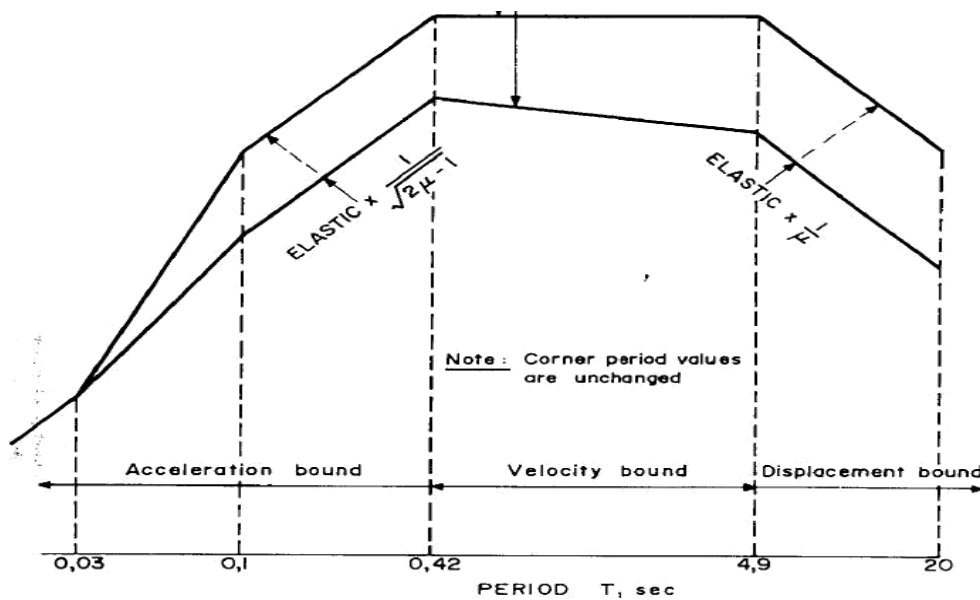
Figure 2.10; Transformation from elastic to elastic-plastic design spectrum (TMH7; 1983)

10

2.7 Methods of analysis provided in TMH7

TMH7 provides four different force-based methods of analysis to determine the seismic forces on bridges subjected to earthquake action. It sets out the minimum requirements applicable to all bridges in South Africa. The methods included in TMH7(1983) are the static analysis method, equivalent horizontal static force method, response spectrum analysis and dynamic analysis method. TMH7 does not provide specifications for static nonlinear analysis methods (e.g pushover analysis method) due to the complexity of carrying out calculations using those methods. However, those methods have proven to be very useful for the analysis and design of complex bridge structures and can be simulated easily using computers. Moreover, TMH7 does not make provision for displacement – based methods which have gained popularity worldwide and are believed to be more economical and less stringent than the traditional force-based method. According to TMH7(1983), the choice regarding the applicability of each method should be based on expected seismic intensity levels and the susceptibility of the bridge to seismic action. A brief description of the different methods is provided below.

2.7.1 Static analysis method

The static analysis method provides the minimum requirements for any bridge structure in South Africa. The method is an approximation method and does not accurately simulate the dynamic effects induced by an earthquake. The use of this method ensures that the designed bridge structure is capable of resisting the minimum specified static lateral forces which are directly related to the properties of the bridge structure and the seismicity of the region (Chopra, 2017). The method specifies the formulas to determine the base shear force as well as the distribution of lateral loads based on the estimated natural vibration of the structure. According to TMH7(1983), the seismic design of bridges using the static analysis method ensures that the bridge has nominal capacity to resist the effects of an earthquakes. For this method, the total nominal horizontal force is determined using equation 2.

$$F_{eq} = k_f \left(\sum_{i=1}^{n} g_{di} + \sum_{j=1}^{n} g_{sdi} \right) \qquad\qquad (2) \quad \text{(TMH7,1983)}.$$

Where k_f = 0.02 if the structure is founded on rock material or a firm subsoil with bearing capacity above 400kpa.

= 0.04 for structures founded on rock material with bearing capacity between 100kpa-400kpa.

= 0.06 for structures founded on piles in soft layer materials with bearing capacity below 100kpa.

= dead load of portion of structure.

= superimposed dead load of portion j of structure

In the static analysis method, the nominal horizontal force caused by the bridge superstructure is applied at the height of the centre of gravity and distributed along its length in terms of the distribution of its mass. The resultant horizontal force of the bridge substructure must be applied in accordance with triangular distribution, increasing linearly in the vertical direction or two thirds from the base.

2.7.2 Equivalent horizontal static force method

This analysis method is adopted from the Canadian national building code of 1980. The method entails the assessment of the equivalent static horizontal force which would induce stress effects equivalent to those induced by a real earthquake. This method is applicable to both bridges with low susceptibility to seismic action and those in which class iv intensity (table 2.3) will not be exceeded. The equivalent horizontal static earthquake force (F_x) is determined using equation 3.

$$F_x = AS\zeta If m_x h_x \left(\frac{\sum_{i=1}^{n} m_i}{\sum_{i=1}^{n} m_i h_i} \right)$$ (3)

Where   A = horizontal ground acceleration.

S = Seismic response factor = $\frac{0.5}{\sqrt{T}}$ but ≤ 1.0

T = Fundamental period of vibration. (seconds)

ζ = numerical factor taking into account damping, ductility, energy dissipation etc.

f = foundation factor.

$\sum_{i=1}^{n} m_i$ = mass of dead load + superimposed load of structure considered divided into n portions.

h_i = Height above base.

2.7.3 Response spectrum analysis

The response spectrum analysis method simulates the structural response of single degree of freedom structures to seismic excitation. The method can either be applied using hand calculation for small bridges (e.g. pedestrian bridges) or using computerized methods on large bridges. TMH7 recommends the use of the deformation, pseudo-

acceleration and pseudo-velocity design spectrum (figure 2.8) for the application of this method. The Quasi-dynamic analysis method is currently the most dominant method used for the design of new structures as well as the safety evaluation of existing structures against future earthquakes.

2.7.4 Dynamic analysis method

The dynamic analysis method is a more rigorous method used in the analysis and design of bridges for seismic excitation. TMH7 recommends that the method be used only on exceptional or major bridge structures which are deemed to be vulnerable to adverse seismic effects. For this method, the bridge is subjected to accelerograms of recorded earthquakes in the region. Due to a lack of recorded earthquake data in South Africa, the South African Bridge code makes use of ground motion data of earthquakes recorded on other continents such as the Aomori California earthquake of 1952, the Ocurido Japan earthquake of 1972 and the Paciuma Dam San Fernando earthquake of 1971. The application of this method requires the use of a suitable computer program such as ANSYS in order to perform a mode superposition analysis.

2.8 Digital image correlation (DIC)

Digital image correlation is a full noncontact image analysis method used to measure strains and deformations. The method was originally developed to measure strains on mechanically loaded test specimen surfaces in solid mechanics (Sudarsanan et al., 2019, Sutton et al., 1983). Over the years, developments in electronic engineering and CMOs sensor technology has resulted in the application of the DIC technique to solve a variety of problems encountered in engineering such as the measuring of strain and displacement during indirect tension test (Kim & Wen, 2002), bridge deflection measurement (Yoneyama et al, 2007) and the influence of compaction aggregate gradation in AC mixtures (Yue and Morin, 1996). The technique has gained popularity due to the ease with which measurements can be performed. Moreover, the use of digital image correlation has proven to be a useful, flexible and cost-effective tool compared to conventional measurement methods such as the use of strain gauges (Sudarsana et al., 2019). Digital image correlation makes use of the analysis of a large number of images taken from a test specimen during the test. The displacement of one or more points is measured directly by comparing the first image (acquired before deformation) with the image acquired after deformation. The computation of the displacements of a point of interest $P(x, y)$ requires a square reference subset of $N \times N$ pixels in the undeformed image to be chosen and its location in the deformed image can then be determined. Once the location of the reference subset is determined in the deformed image, the displacement of the reference subset can be

approximated using a normalized cross correlation coefficient (S) defined by equation 4 (Tain et al., 2013).

$$S\left(x, y, u_x, u_y, \frac{\partial u_x}{\partial x}, \frac{\partial u_x}{\partial y}, \frac{\partial u_y}{\partial x}, \frac{\partial u_y}{\partial y}\right) = 1 - \frac{\sum I_u(x,y) I_d(x^*, y^0)}{\sqrt{\sum I_u(x,y)^2 \sum I_d(x^*, y^*)^2}} \qquad (4)$$

Where; u_x & u_y = displacement components at the centre of the subset,

   I_u & I_d =represent the grey levels of the undeformed and deformed images, respectively,

   (x, y) & (x*, y*) = coordinates of a point on the subset before and after deformation, respectively.

(x*, y*) and (x, y) are related by equation 5.

(x*, y*) and (x, y) are related by equation 5.

$$x^* = x + u_x + \frac{\partial u_x}{\partial x}\Delta x + \frac{\partial u_x}{\partial y}\Delta y$$

$$\qquad\qquad (5)$$

$$y^* = y + u_y + \frac{\partial u_y}{\partial x}\Delta x + \frac{\partial u_y}{\partial y}\Delta y$$

This method of analysis approximates the displacements to an accuracy of one pixel with zero gradients at first iteration. After the first iteration, the process then uses the Newton – Raphson method to search for the displacement and displacement gradient (Yoneyama et al.,2007).

2.9 Application of FEA in Bridge Engineering.

Over the years, several bridge analysis methods have been developed and implemented. According to scholars such Drosopoulos et al., (2006), one of the most accurate method is the application of finite element analysis method. Finite element analysis on bridges was first carried out by Towler and Sawko in their study of masonry arch bridges (Page, 1993). FEA methods at the time were very simplistic and only made use of the linear elastic, small deflection analysis methods in analysing bridge structures. Over time, FEA software has become more advanced. Software's incorporating higher-order methods are becoming more common in the industry due to the high capability to incorporate nonlinearities to account for realistic stresses and deformations influencing the performance and service life of a bridge (Marefat et al., 2017). Aspects that can be

incorporated into an advanced FEA model in addition to material and geometric nonlinearities to assess the structural integrity of a bridge include; the response of concrete or steel to the weight of the bridge itself, as well as to traffic, wind, water, temperature fluctuation, corrosion, and even time.

FEA works by breaking down a large complex problem into smaller simpler finite elements. The governing equations for each element are calculated and then assembled to give a system of equations, which describe the behaviour of the body as a whole. For the finite element analysis of the bridge, the system equation takes the form shown in equation 6.

$$[F] = [K] \, x \, [u] \qquad\qquad (6)$$

Where:

[K] = Stiffness matrix

[u] = Displacement vector

[F] = Force vector

The steps followed in carrying out an analysis using FEA software are as follows:
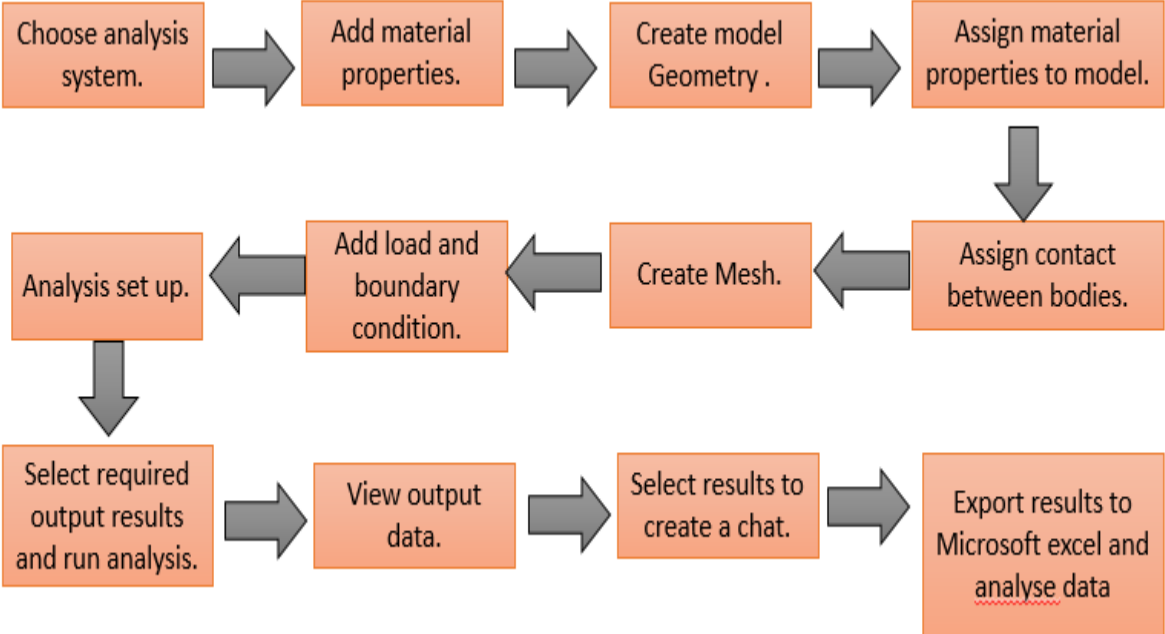
Figure 2.11; procedure to followed in carrying out analysis using FEA software.

2.10 Case study (Åby river bridge)

A study involving measurement and evaluation of the structural behaviour of an open steel truss railway bridge (Åby river bridge) was conducted by the Luleå University of Technology. The study involved the destructive testing of the Åby River bridge to failure in order to assess the structural behaviour of the bridge. The Åby river bridge was structurally similar to the Groot Olifants river Bridge, hence conclusions are drawn from the study conducted by the Luleå University of Technology to support the observed behaviour of the Groot Olifants river bridge. The Åby bridge was a 32m steel truss railway bridge with a width of 5.5m Figures 4-5.

Figure 2.12; Åby bridge (photo by Thomsa Blaksvard)
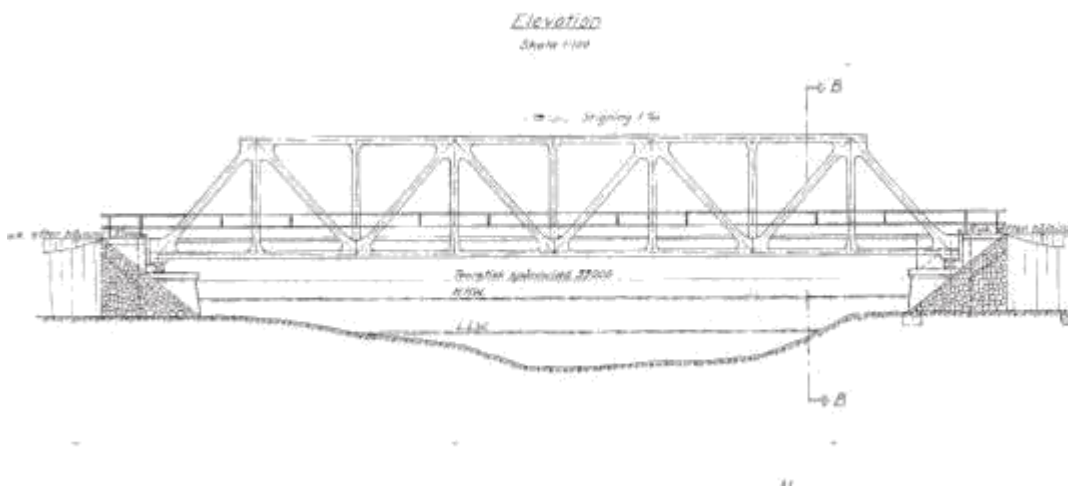
Figure 2.13; Drawing of the Åby River bridge (Haggstrom, 2014)

The Åby bridge differs from the Groot Olifants bridge in that the truss is not inverted. The bridge was built in 1957 and was tested to failure in 2012 to study the structural behaviour and the remaining load carrying capacity of the bridge (Blanksvärd et el., 2014). The bridge was designed for an ultimate load carrying capacity of 25 tones/axle corresponding to F46 type locomotives (Appendix C). Like the Groot Olifants Bridge, the Åby River bridge, connections were riveted connections. In performing the failure test, the Åby bridge was placed on temporary concrete supports. Fourteen Linear Voltage

Displacement Transducers (LVDTs) were installed on the main truss to measure the displacements of the truss. Strain gauges and temperature measuring sensors were installed on the truss as well as the stringer beams and crossbeams. The sensors were connected to the MGC data acquisition system, which collected the data and stored it on a computer. A static load was applied and kept constant for ten minutes before unloading using oil pressure jacks. Four different load scenarios consisting of 1000kN, 1320kN, 1600kN and 1800kN loads were initially applied. A full-scale test to failure cannot be performed on the Groot Olifants river bridge as it is still in use, therefore failure of the bridge will be conducted using FEA and the results will be compared against the failure results of the Åby River bridge.

2.11 Chapter summary.

In this chapter, the contributions made by various researches regarding the seismic analysis of bridges in South Africa is presented. The chapter first provides an overview of the seismic risk of South Africa. It then goes on to look at seismic induced modes of failure in bridges, focusing mainly on the bridge substructure and bridge superstructure. The impacts of bridge failure are then analysed using the Morandi bridge collapse as a case study. The chapter further provides a detailed research of the different methods of analysis found in TMH7 (1983). A brief review of the digital image correlation technique is provided. The chapter ends with a summary of the application of finite element analysis methods in bridge engineering. The knowledge gained in this chapter is fundamental for the understanding of the application of the computer programmes used in chapter 4. The chapter fundamentally ensures that the reader understands the theories that the computer programmes used in this investigation are based on. This enables the accurate modelling of the steel bridge and ensures that the reader makes informed judgements in the analysis of the results obtained in chapter 5.

CHAPTER 3

Methodology

3.1 Introduction

The aim of the research was to assess the structural performance of the Groot Olifants River bridge, considering mainly the ultimate load carrying capacity, the structural response to seismic excitation, as well as the failure mechanism. This chapter presents a detailed numerical analysis which incorporates the various load cases as well as the methodology used to carry out the field tests. The results from the field tests were used to calibrate and validate the accuracy of the numerical model by evaluating the maximum deflections measured on site and comparing the experimental results with computational results. All aspects regarding field tests performed on the Groot Olifants river bridge are provided in this chapter.

3.2 Bridge description.

The Groot Olifants River bridge was designed and constructed in 1887. The bridge superstructure consists of three identical structural steel inverted trusses with the railroad on top of the truss (figure 1). Each truss forms part of the main girder of the bridge and has a span of 32 meters, a width of 3.48m and a height of 0.9m. The total length of the bridge is 96m (figure 2). The main truss system of the Groot Olifants river bridge was fabricated using a combination of channel sections, plates and steel angles. The trusses are connected by cross beams as well as vertical and horizontal bracing.

Figure 3.1; Groot Olifants River bridge

According to the design, the truss channels and angles resist all axial forces while the bracing members provide stability. The cross beams (which provide lateral stability) connect the two trusses every 3,12m. All the truss connections consist of rivet connections as illustrated in figure 3,2.

Figure 3.2; Typical connection on the Groot Olifants river bridge

The bridge superstructure is supported on two double-arched coursed masonry abutments and two piers. One of the piers was subsequently encased in mass concrete. All the abutments and piers are supported on pad footings. The bridge superstructure is connected to the abutments (at either ends) using a pinned plate bearing that allows only for rotational degrees of freedom, while it is supported at the piers by unidirectional plate bearing which allow movement in the longitudinal direction. The Groot Olifants river bridge was inspected in February 2019 before the field tests were conducted and found to be in good condition according to the MICA inspection specifications.

3.3 Methodology

Techniques such as the ambient vibration monitor and the forced vibration test have been widely used to investigate the structural response of various structures in different parts of the world e.g. assessment of the structural integrity of steel foot bridge (Bayraktar et al., 2007, Živanović et al., 2006) and the assessment of two storey masonry house (Vestroni et al., 1996). However, in South Africa, it is considered impractical and too expensive to conduct full scale seismic excitation experimental tests using those techniques to collect data from over 5000 bridges. Therefore, it was decided that for this research, numerical analysis (FEA) would be used to investigate the structural response of the bridge to seismic excitation.

FEA is commonly recognized as both an effective and efficient technique for the evaluation of the structural behavior of old structures (Aguilar et al., 2017, Aktaş & Turer,

2015, Betti & Vignoli, 2008, Sánchez-Aparicio et al., 2014, Terzi & Ignatakis, 2018, Taliercio & Binda, 2007, Vercher et al., 2015). The research was carried out in two parts. In part one, full scale static load tests were conducted on the Groot Olifants river bridge to measure the maximum deflections. In part two, a numerical (FE) model was developed. This required that the various material properties, geometric properties as well as boundary conditions be accurately determined and incorporated into the FE model. This section of the paper provides a detailed description of how the various parameters were determined as well as how the FE model was calibrated and validated to ensure accuracy and reliably of the results obtained.

3.3.1 Visual inspection

Field-tests (mica inspections) were conducted to determine the structural condition of the bridge superstructure. A detailed site investigation was conducted on the bridge to qualitatively evaluate the structural condition, detect any defects (corrosion, deformation, failed steel members etc) on the structure in accordance with the Mica Inspection specifications and to determine the geometric parameters and boundary conditions. Binoculars and a cherry picker were used to inspect inaccessible areas such as bearings on supporting abutments and structural members not within reach of the inspector. It was observed that the bridge was still in good condition, however, slight corrosion on some of the main truss members was observed.

3.3.2 Field test using digital image correlation techniques

Field tests were performed using the 44D locomotive and DIC techniques. According to Yoneyama et al., (2007), in order to carry out DIC usefully and accurately, the image acquisition speed of the camera must be high enough to reproduce the real-time dynamic response of a bridge. A Canon EOS 550D single lens reflex camera equipped with 18-megapixel APS-C CMOS sensor and a 50mm f/1.8 STM lens was used. The EOS 550D camera was connected to a laptop via a USB cable and placed on a tripod (figure 3-4) three meters away from the bridge. The bridge stringer beams were instrumented with Digital image correlation target at selected points as shown in figure 3-5. The bridge was then loaded with 44D locomotives positioned at three different locations to evaluate the different load cases as illustrated in figures 3-6 to 3-10. The tripod bubble level was used to ensure that the camera was leveled and the optical axis of the camera lens stayed normal to the target point. A CSP 2008 controller was used to process data from Micro-Epsilon. Microsoft Excel was used to analyse the data obtained from the DIC measurements. The used 44D locomotives have an axle load of 21.6 tonnes/ axle. In Appendix A, the 44D locomotive specifications are provided. The vertical deflections

were determined using Digital Image Correlation (DIC) techniques as specified in section 2.7. The measured vertical displacements were used to calibrate the numerical model.

Figure 3.3; DIC set up.

Figure 3.4; digital image correlation points

Figure 3.6; Field load position 1 (first bougie of loco 1)
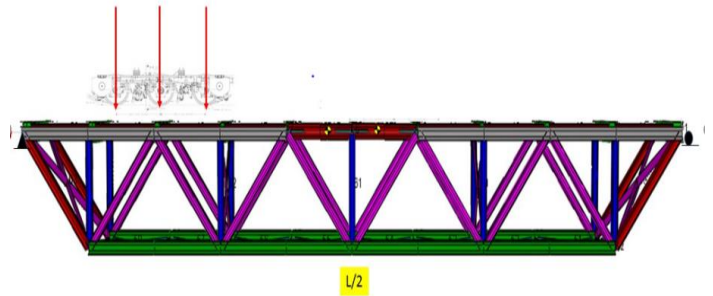
Figure 3.5; Model load position 1 (six-point loads at the start of the bridge)."
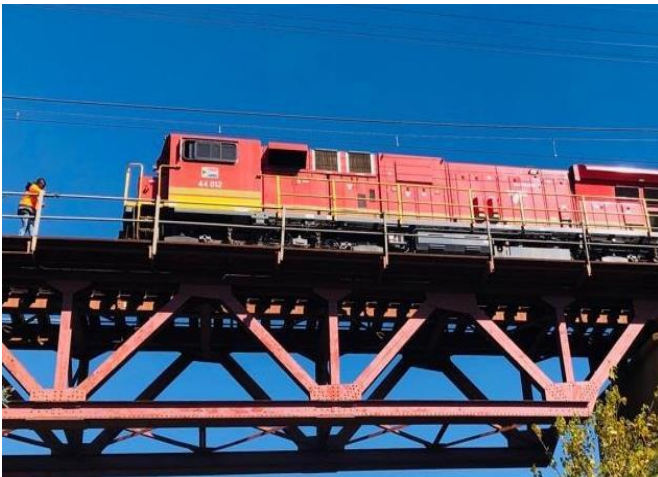
Figure 3.10; Field load position two (first and second bougie of the first loco)
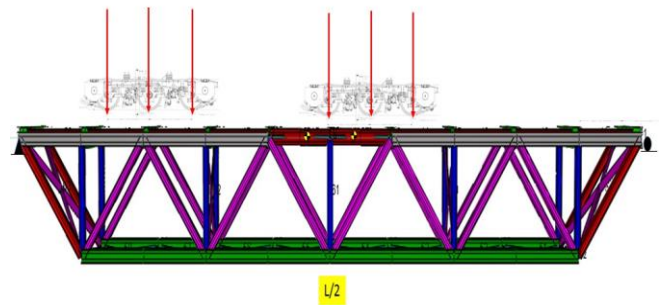
Figure 3.8; Model load position two (6-point loads at the start of the bridge and 6-point loads at the middle of the bridge)
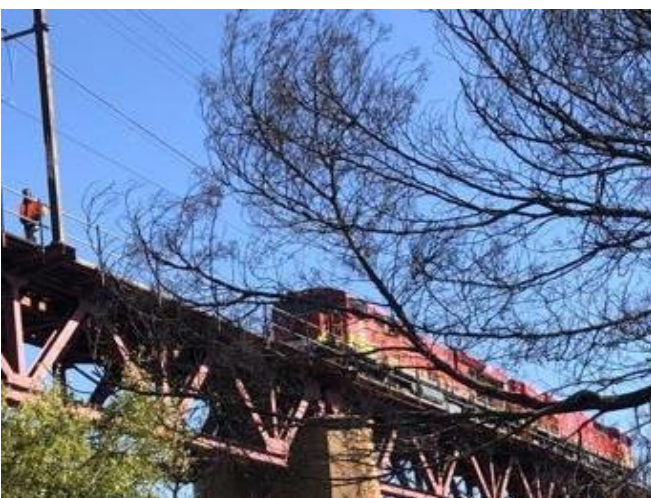
Figure 3.9; Field load position 3 (coupler, loco1 and first bougie of loco 2)
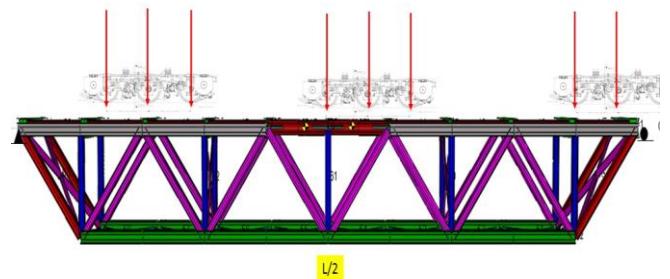
Figure 3.7; Model load position 2 (6-point loads at the start, middle and end of the bridge respectively.

3.4 The computational mechanics experiments

The Groot Olifants river bridge was modelled using one dimensional beam elements. The geometry was created using ANSYS (version 19.2) DesignModeler. Cross-sectional properties were assigned to each beam element. The structural system is that of a 3D truss. The applied boundary conditions consist of a fixed support at one end of the bridge and pin support at the other end. The finite element model consisted of 14235 mesh elements. Figure 8 shows the FEA model. The FE model created before the field tests was improved using the experimental measurements obtained from the DIC tests to develop the final calibrated model to ensure it produced accurate and reliable results.
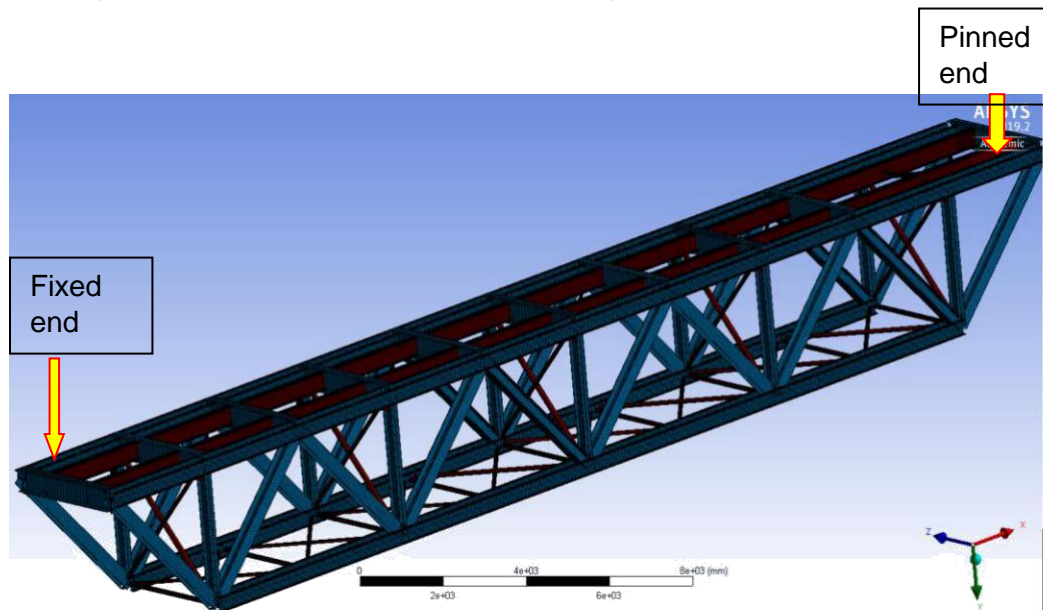
Figure 3.11; FEA model.

3.4.1 Assumptions

The following assumptions were made in the modelling of the Groot Olifants river bridge,

1) The yield stress for the type of steel used was taken as approximately 265 MPa.
2) The Young's Modulus (E) applied to the steel for analysis was 200 GPa,
3) All loads and reactions are applied only at joints.
4) An earthquake is unlikely to occur coincidently with high wind or while a train is running on the track.

3.4.2 Model limitations

Although ANSYS workbench is considered an excellent instrument to assess the structural response of steel bridges subjected to seismic loads, some limitations were encountered. Several clear simplifications were incorporated in developing the numerical model presented in section 3.4.1. Those simplifications are justified by the need to

minimise the analytical complexities and maximum numerical efficiency during analysis. The restrictions and simplifications are as follows;

(i) The final models adopted did not consider the effect of the physical condition of the structural steel on site. The effect of corrosion and the remaining life of the steel was not considered.

(ii) The ground motion of the abutment was also not considered during the assessment of the bridge. Seismic loads were applied directly to the bridge superstructure whereas during an earthquake, seismic loads are applied to the foundation and transferred to the superstructure.

(iii) In the numerical analysis, a single span (of the three non-continuous spans) was modelled due to computational limitations instead of all modelling all three spans.

3.4.3 Resolving model limitations.

To ensure that the limitations of the numerical model do not greatly affect the results obtained, the model was examined three times. Another finite element software, Siemens Nx, was also used to check if some of the results obtained correlated well. The accuracy of the model was also verified by comparing computational results with field results. The model results of the Groot Olifants River Bridge were also compared with the results of Aby River Bridge obtained from literature to study and validate the structural behaviour of the two similar bridges as discussed in sections 3.7 and 4.6.

3.5 Eigenmode analysis

Modal analysis was performed using ANSYS workbench to determine the bridge Natural frequencies and mode shapes. The natural frequencies and mode shapes of a structure are essential modal characteristics required for any dynamic analysis as they affect the dynamic response of a structure, as well as the generation and transmission of vibrations (Bruno et al., 2014, Meena et el., 2013, Rao, 2004). The modal analysis provides an indication of the frequency range in which the bridge will be more sensitive to vibration. FEA can be used to predict modal shapes and frequencies, decrease the cost of manpower and material resources in modal test (Guangming et al., 2011). The natural frequency is the main consideration in designing structure to resist earthquake
loading. However, the modal shapes and frequency obtained from FEA are often prone to errors arising from simplified assumptions made in the modelling of the structures, as well as parameter errors due to structural damage and uncertainties in the material and geometric properties (Ren, 2004, Guangming et el., 2011). Nonetheless, in this study, experimental load tests results were compared with the computational results to verify

the accuracy of the model, which ensures the accuracy of the modal frequency and mode shapes obtained from the FEA model.

3.6 Seismic analysis

3.6.1 Response spectrum analysis (RSA)

Single point response spectrum analysis was performed to determine the structural response of the bridge to seismic excitation. The Rosenblueth's Double Sum Combination (ROSE) method was used with 10% missing mass. The first fifty modes from the modal analysis, with a total mass participation factor of ±90% were used in the RSA. A design spectrum from the deformation, pseudo-velocity, and pseudo-acceleration spectrum provided in TMH7 with 5% damping ratio (figure 2.8) was used as an input. An assumption was made that an earthquake is unlikely to occur coincidently with high wind or while a train is running on the track, therefore the upstream modal analysis was not pre-stressed by a static analysis.

3.6.2 Dynamic time history analysis

Transient structural analysis by mode superposition using the validated FEA model was carried out to stimulate the effects of an earthquake with a magnitude of 6.87 and peak ground acceleration (Pga) of 0.2. the upstream modal analysis was not pre-stressed by static analysis.

For this analysis, Ground motions (acceleration – time curves) were applied as loading to the supports of the bridge superstructure. This study makes use of earthquake data from an earthquake that occurred in the Southern Part of Italy (Irpinia 1980) due to a lack of comprehensive earthquake data with the required magnitude and intensity for Mpumalanga region. The magnitude of Irpinia earthquake was 6.69 and the peak ground acceleration (g) equal to 0.29 (Motsa, 2018). Figures 3-12 to 3- 14 shows the recorded ground motion (acceleration – time graphs in the three dimensions) for the Irpinia seismic event (Berkley, 2018). The Irpinia earthquake was selected due to available comprehensive PGA and intensity data which are similar to the earthquake magnitudes predicted by Visser and Kijko (2010)
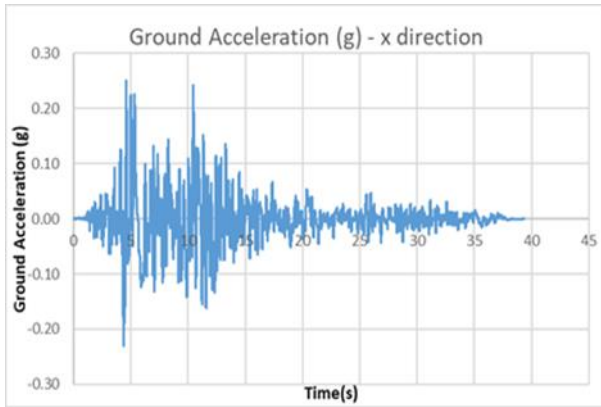
Figure 3.13; X-direction acceleration - time graph from Irpinia earthquake 1980 (Berkley, 2018)
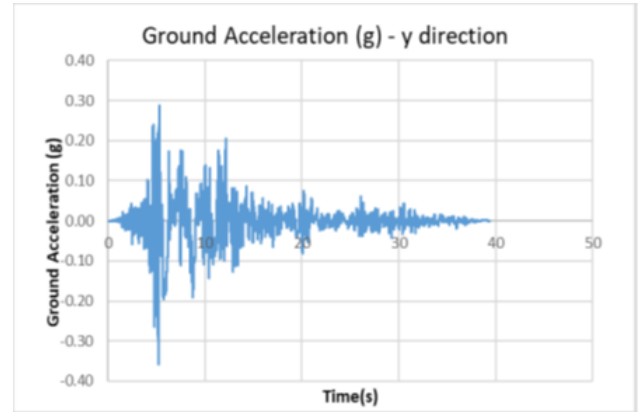
Figure 3.12; Y- direction acceleration time graph from Irpinia earthquake 1980 (Berkley, 2018)
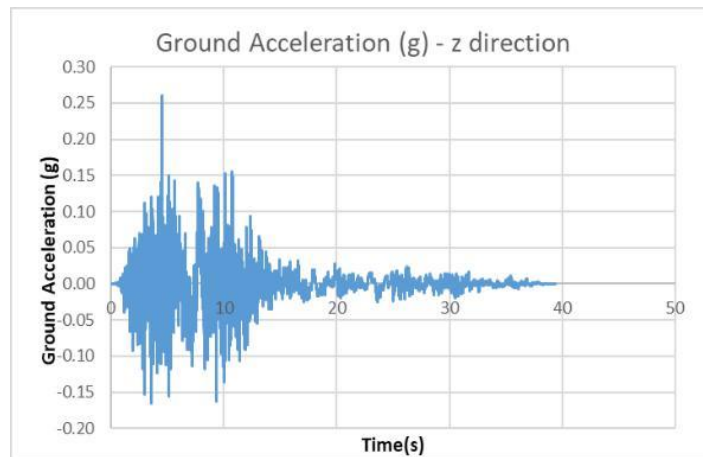
Figure 3.14; Z- direction acceleration - time graph from Irpinia earthquake 1980 (Berkley, 2018)

26

CHAPTER 4
Results and discussion

4.1 Validation of analytical model

The present study investigated the structural response of the Groot Olifants River Bridge to seismic excitation. To validate the finite element model used in the analysis, the vertical deflection results obtained from the field DIC tests were compared to the analytical results obtained from the FEA model. In the FEA computation, the vertical deflections were determined at the same locations where the DIC targets were located as illustrated in figures 3-5 to 3-10. Table 2 shows that the FEA computational results are similar to the DIC experimental results with a maximum variation of 6.6% obtained in load case three. A slight variation between DIC results and the finite element analysis results was expected since in the FEA model, the rails, sleepers and fastening system (which in reality contribute to the bridge stiffness) were not considered. Moreover, in the numerical model, corrosion of the steel as well as the conditions of the rivet connections was not accounted for.

Table 4.1; Comparison of DIC results and numerical results.

Load Position	Field: DIC Vertical deflection (mm)	FEA Model Vertical deflection (mm)	Variance (%)
Loco 1 - First wheel (figure 3.6 -3.7)	-10.989	-10.44	4.90%
Loco 1 and 2 – Coupler (Figure 3.8-3.9)	-13.38	-12.79	4.30%
Loco 2 - First Wheel (figure 3.10-3.11)	-15.857	-16.902	6.60%

According to the bridge code, the maximum vertical deflection for railway bridges must not exceed 1mm per meter of span. Therefore, the maximum deflection of -16.902mm obtained from the FE analysis of the 32m span bridge is within limits (max deflection for 32m bridge is 32mm). Figure 4-1 shows a graphical comparison of vertical deflections measured on site with those obtained from the FEA model. This correlation demonstrates that the Finite Element Model used in this study is an acceptable representation of the Groot Olifants river bridge. Figures 4-2 to 4-4 shows the structural response of the bridge as captured by the FEA simulation.
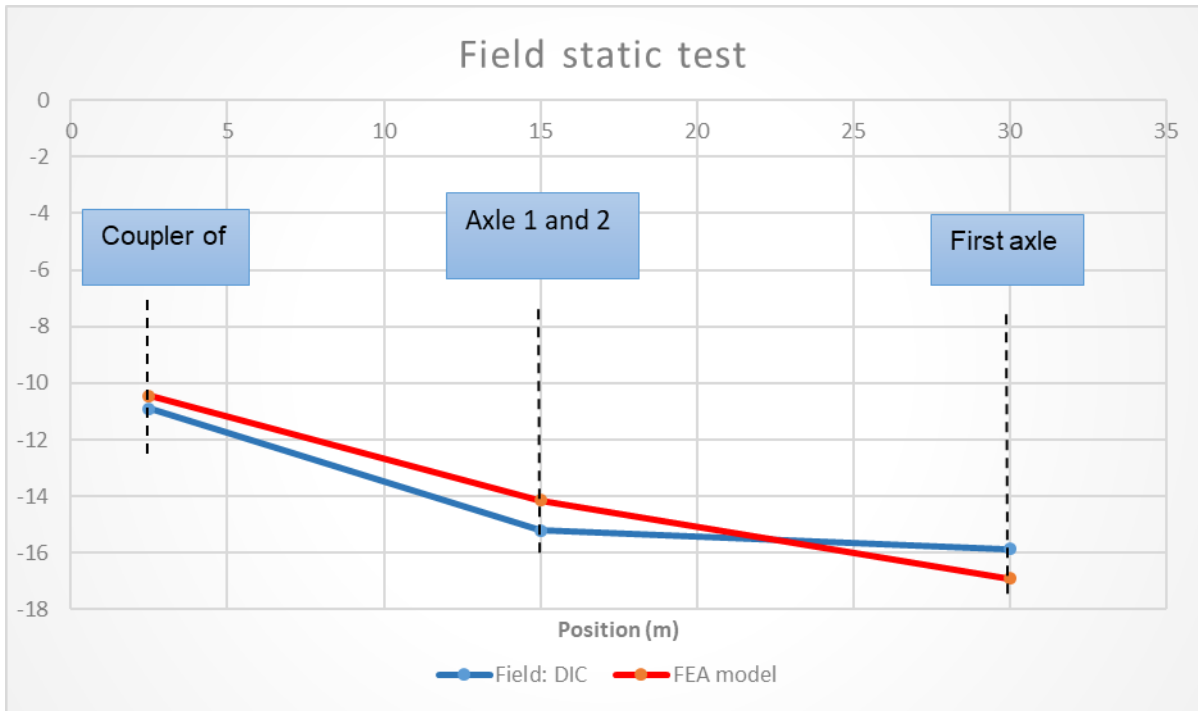
Figure 4.1; Graphical comparison of the Field DIC vertical deflection and FEA model vertical deflections (mm).
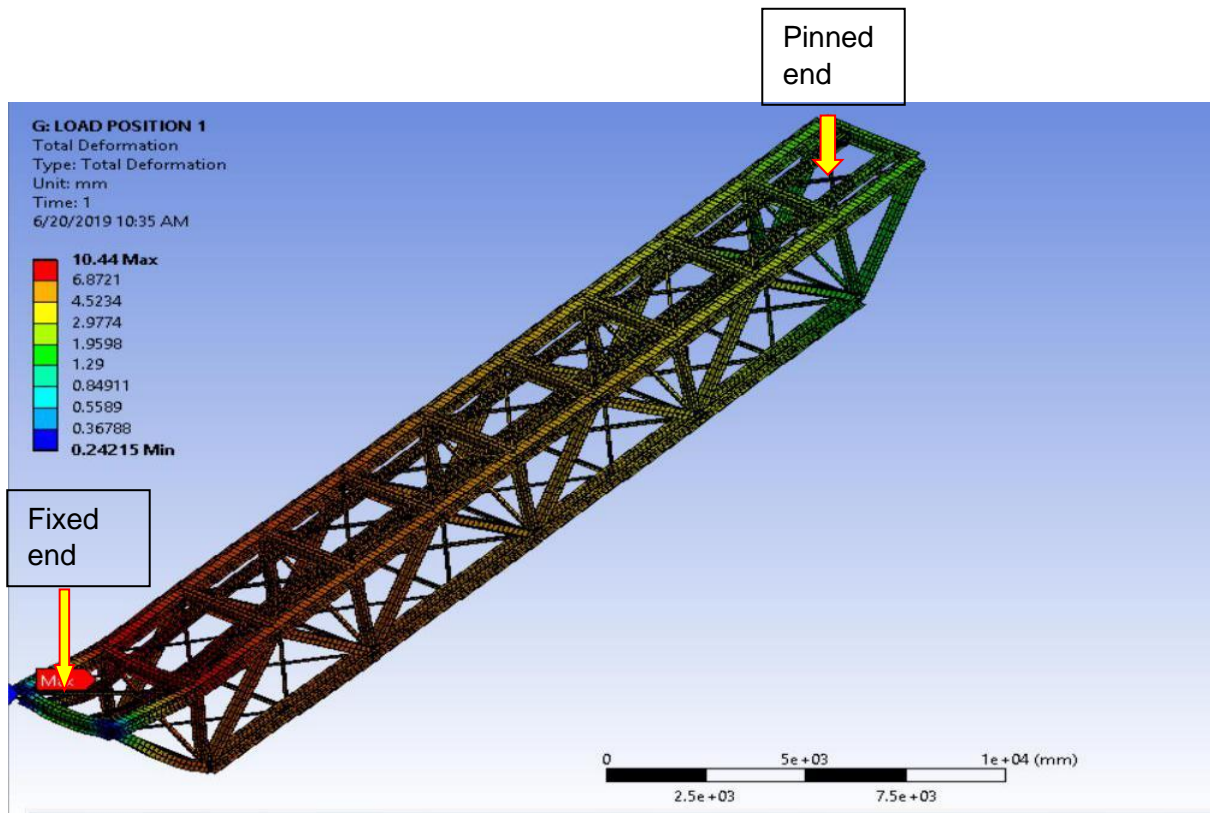
Figure 4.2; Behaviour of the Groot Olifants river bridge subjected to load case 1 (defined in figure 3.7)
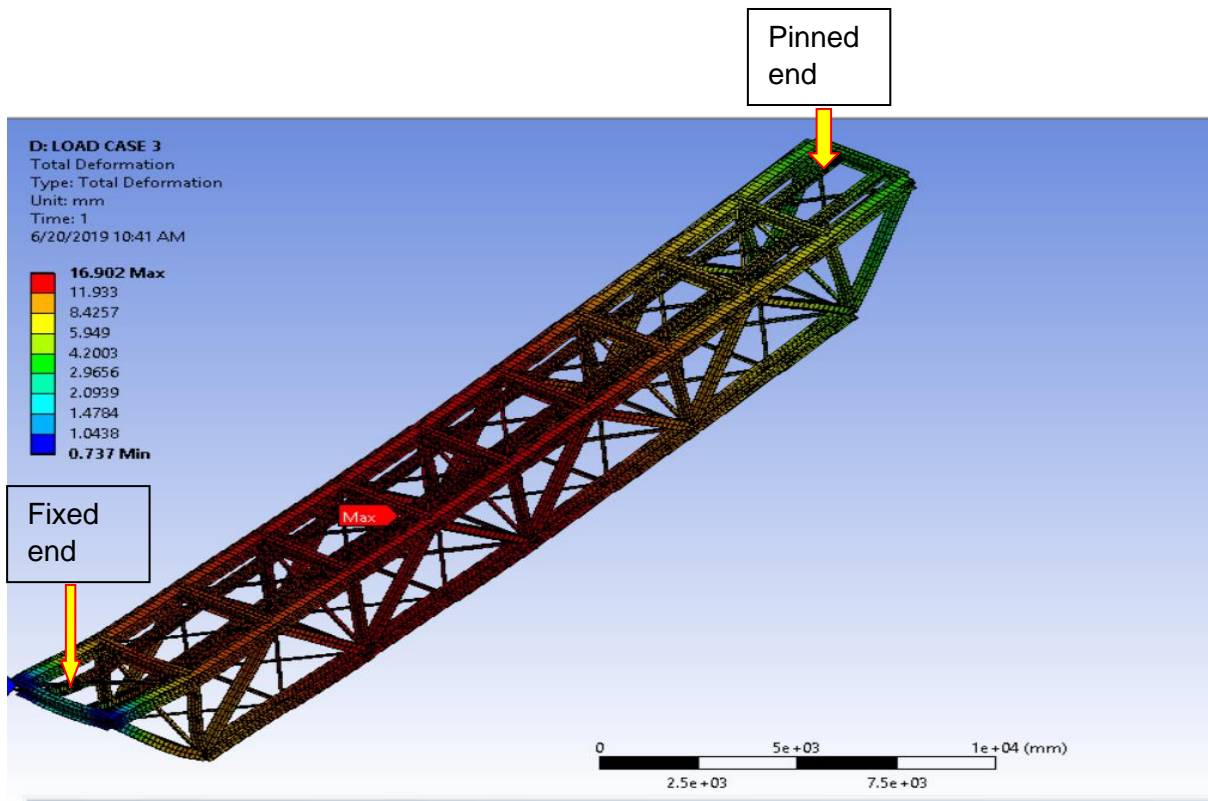
Figure 4.3; Behaviour of the bridge subjected to load case 2 (defined in figure 3.9)
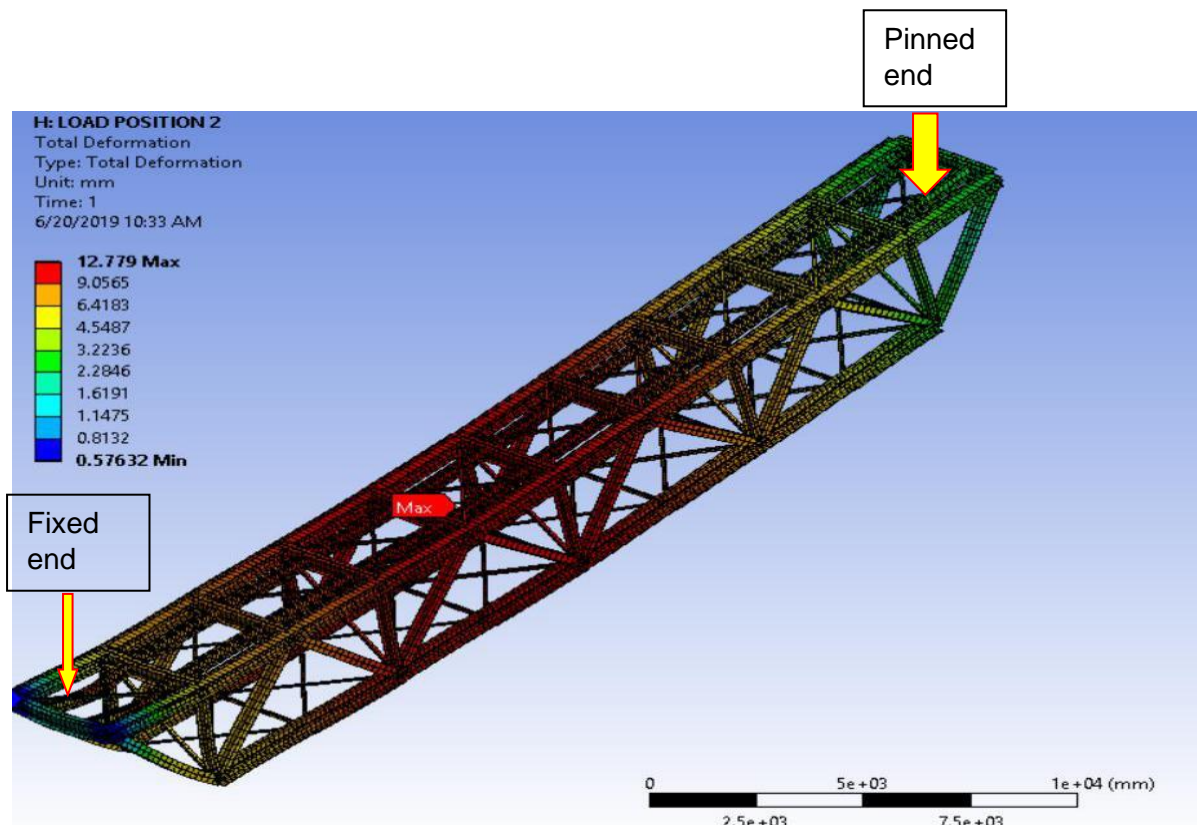
Figure 4.4; Behaviour *of the bridge subjected to load case 3 (defined in figure 10)*

Figures 4-2 to 4-4 indicate that the maximum deflection occurs on the rail barriers. As the load is applied, the rail barriers (Appendix H) are subjected to bending moments while the bracing members on top of the bridge are subjected to compression, causing

them to buckle. The figures further illustrate the manner in which forces are transferred from the point of load application (stringer beams – Appendix H) to the cross beams then to the compression members and finally to the support.

4.2 Modal analysis

After the validation and verification of the finite element model, a modal analysis of the bridge was conducted to extract the modal frequencies and a corresponding mode shape. This analysis provided the first insight into the dynamic behaviour of the bridge. The modal analysis results (modal periods) are the main parameters used in the time history analysis and response spectrum analysis. The results of the first five modes and the corresponding frequencies are shown in Table 4-2. The mode shapes of the first three modes computed in the finite element model are illustrated in Figures 4-5 to 4-7. The principal modal shapes of the Groot Olifants river bridge superstructure include the flexural deformation in the y direction (figure 4-6), transverse translation (figure 4-7) longitudinal translation and the global torsion (figure 4-5)

Table 4.2; Mode frequency and mode shapes description

Mode#	Modal FEA Frequency (Hz)	Mode shape descriptions
1	8.573	Bends in both the top and bottom chords of the truss
2	12.343	In plane bending of the truss bridge about the z axis.
3	13.990	Bending of both the top and bottom chords of the truss in the z axis.
4	16.977	Bending of the bracing members in the x direction
5	18.905	Twisting of the stringer beams.
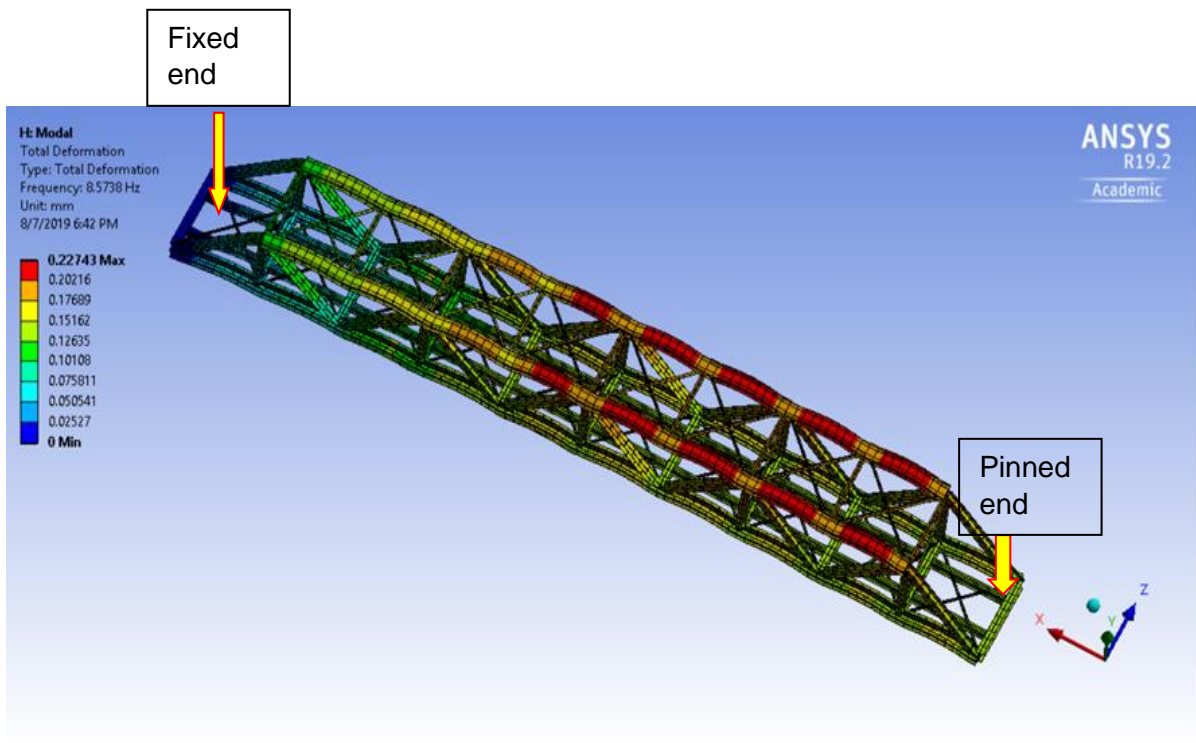
Figure 4.5; First mode shape
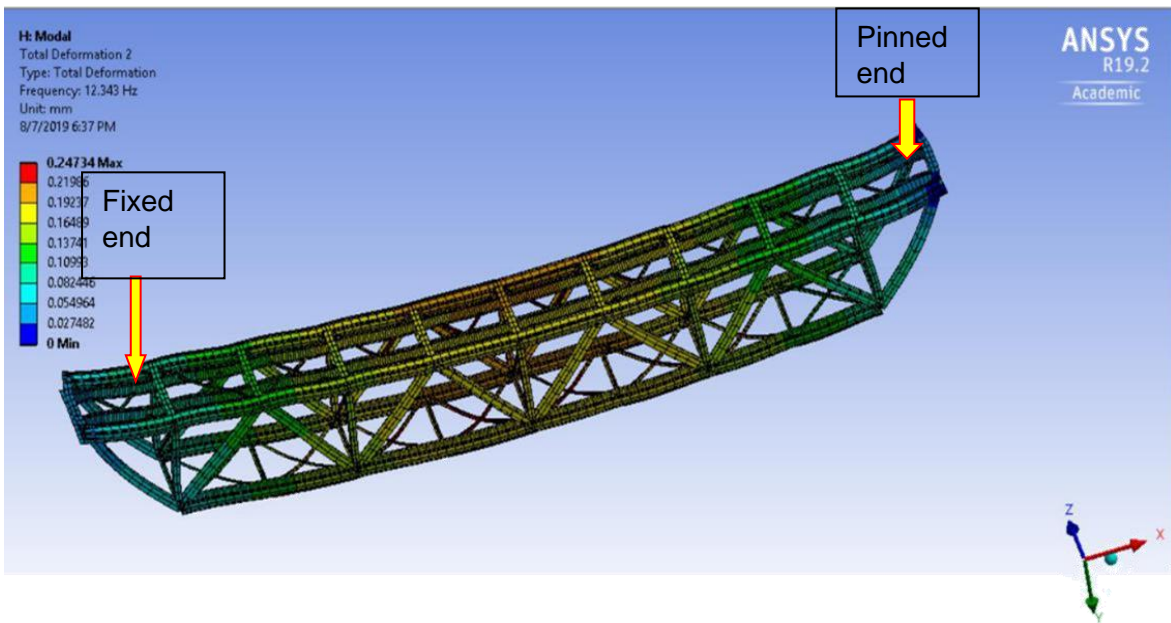
Figure 4.6; Second mode shape
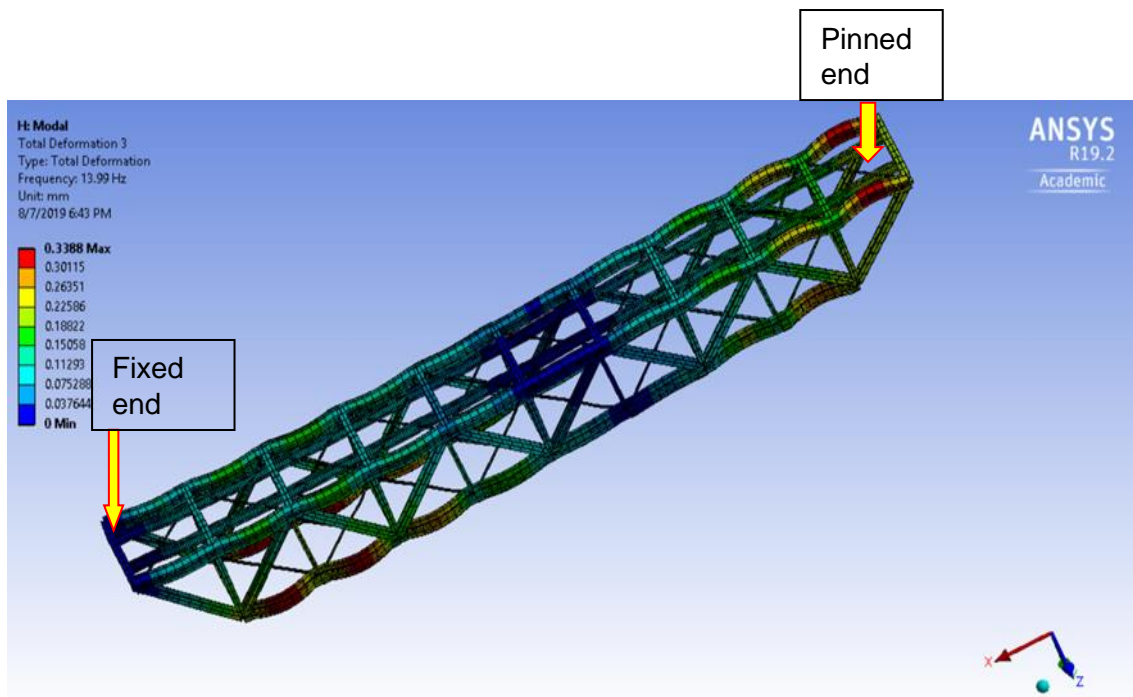
Figure 4.7; Third mode shape

From the results of the modal analysis, it was observed that that different elements of the bridge are activated at different modal shapes as illustrated in figures 4-5 to 4-7. The mode shapes could not be verified as accelerograms could not be installed on the bridge.

4.3 Response spectrum analysis results

In the response spectrum analysis, a mode superposition procedure and the SRSS modal combination method combining the first 50 modes in the modal analysis was used as a first attempt to study the structural response of the bridge to seismic loads. Figure 4,8 indicates that the bridge deflects by a maximum of 6.916mm when subject to the design spectrum as obtained from TMH7. The maximum deflection occurs in the bottom chord of the main truss. The deflection of 6.916mm is less than the maximum allowable deflection (32mm) as prescribed in TMH7.
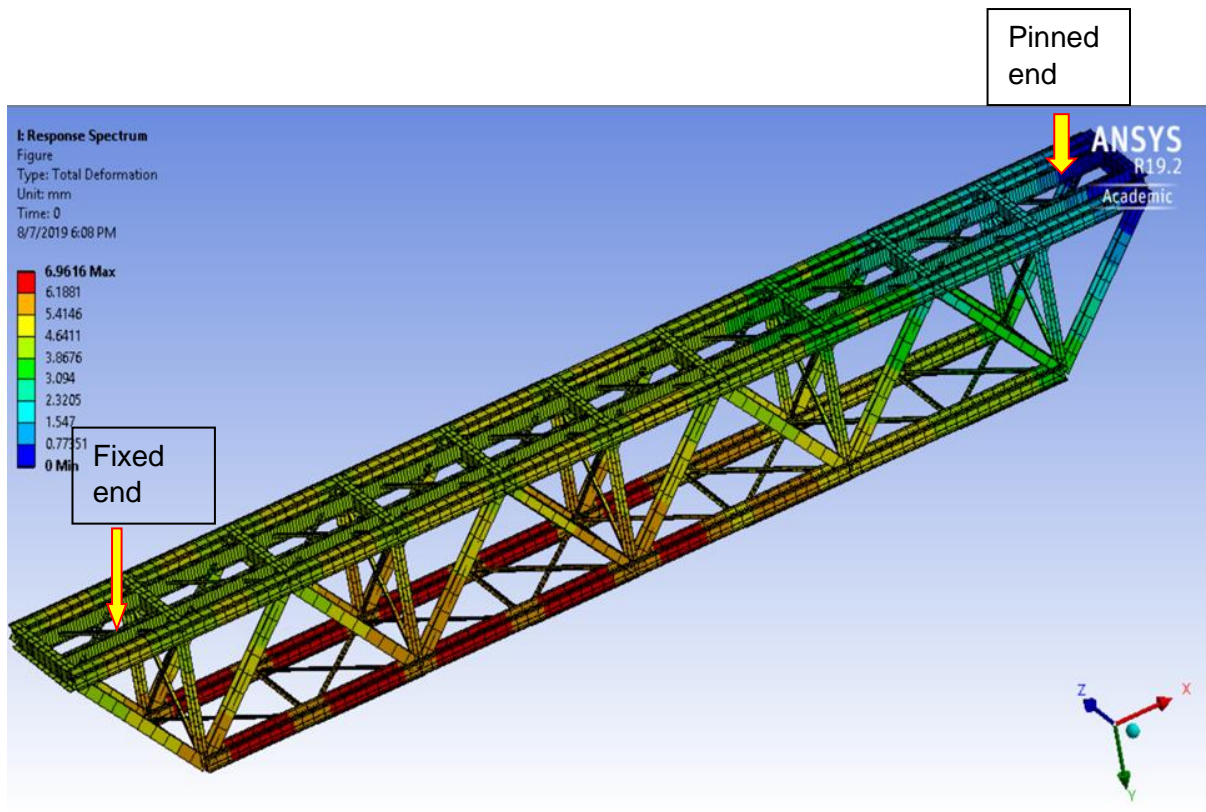
Figure 4.8; Response spectrum results

RSA is a fast method used as a quick estimator to determine failure of the bridge. The method is used to determine the possibility of failure occurring when the bridge is subjected to a moderate intensity earthquake; the stresses in the various members of the bridge superstructure were determined and compared to the material yield strength. From the comparison, it can be noted that the tensile stresses in the main structural members are less than the material yield stresses when subjected to the design spectrum. The above discussion indicates that although the bridge was not designed for seismic loads, the bridge components can resist seismic ground motions predicted by the bridge design code.

4.4 Dynamic time history Results

From the analysis of the Mode-Superposition Transient Structural analysis, it was observed that when the bridge is subjected to seismic excitation it oscillates in the direction of the seismic load application. For this study, the seismic loads were applied in the X, Y, Z directions on the fixed support and in the X, Y directions on the pin support. This resulted in the bridge oscillating in the three directions thus experiencing maximum and minimum deflections corresponding to each peak ground acceleration. The applied seismic ground motion data (as illustrated in Figures 3-12 to 3-14) indicates that four acceleration peaks were encountered at about 4.8s, 7.0s, 10.4s and 15s respectively. It was expected that those peaks would trigger higher deflections in the bridge superstructure.

The first maximum deflection (11.023mm) on the bridge superstructure was observed at 4.4 seconds (Figure 4,9). This corresponds to the time at which maximum ground acceleration in the x direction was experienced. Figures 4-9 to 4-12 further indicate that the maximum deflections are experienced at the cross-beam support where the bearings of the bridge are located. This was attributed to the fact that acceleration base excitation was applied at those points.

In figure 4-9, the maximum deflection occurs at the fixed support end. This is due to the fact that the x direction ground acceleration was applied at the fixed support only.
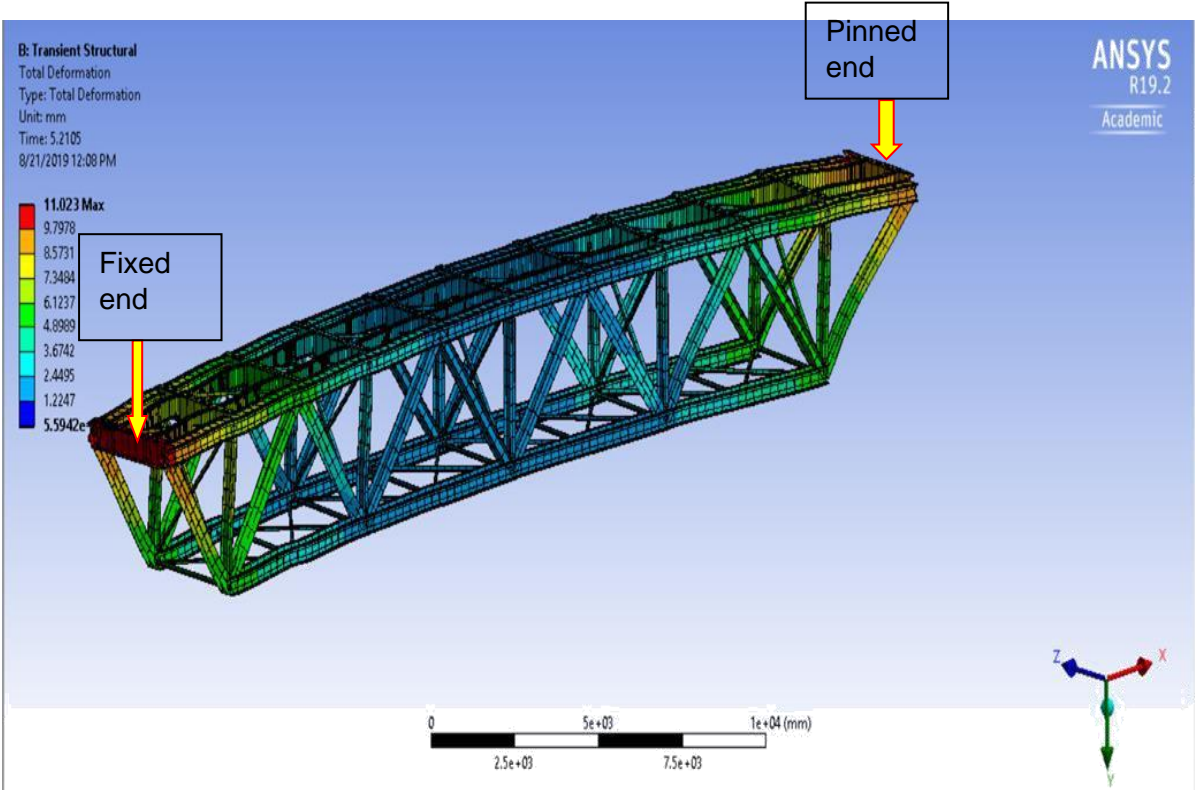
Figure 4.9; Deflection of bridge due to first peak acceleration

The second maximum deflection of 16.71mm was experienced by the bridge superstructure due to the second peak ground acceleration at 7.0s (Figure 4, 10). The results indicate that the first two maximum deflections (11.023mm and 16.71mm) experienced by the bridge due to the peak ground accelerations are less than the maximum allowable deflection (32mm) as specified in the TMH7.
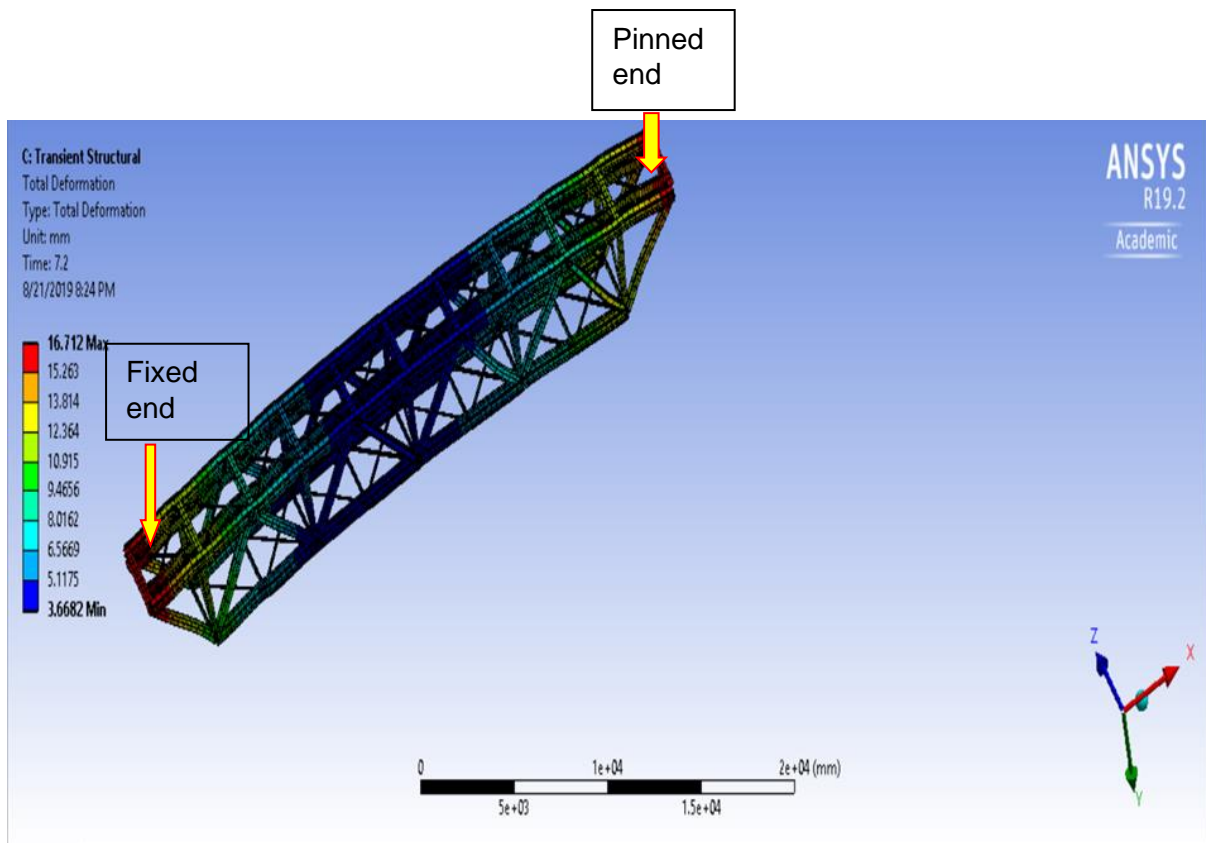
Figure 4.10; Maximum deflection due to the second peak ground acceleration at 7.0 seconds

The bridge superstructure experiences an absolute maximum deflection of 91.482mm at about 10.4 seconds (figure 4-11). This is the highest deflection experienced by the bridge superstructure when subjected to the applied seismic loads. At the point of absolute maximum deflection, it is observed that the there is a peak in the ground acceleration in all three directions (X, Y, Z) as shown in figures 3-12 to 3-14. After the absolute maximum deflection, the bridge oscillation reduces. The final maximum deflection of 41.926 is experienced at 15 seconds (figure 4-12). The deflection at 15 seconds is smaller compared to the previous deflection at 10.4 seconds even though the ground acceleration peaks in all three directions. This is attributed to the fact that the peak acceleration is much greater in all three directions (X,Y,Z) at 10.4 seconds compared to that at 15 seconds. It is further noted that the last two maximum deflections (91.482 and 41.926) are both greater than the maximum allowable deflections recommended in the bridge code.
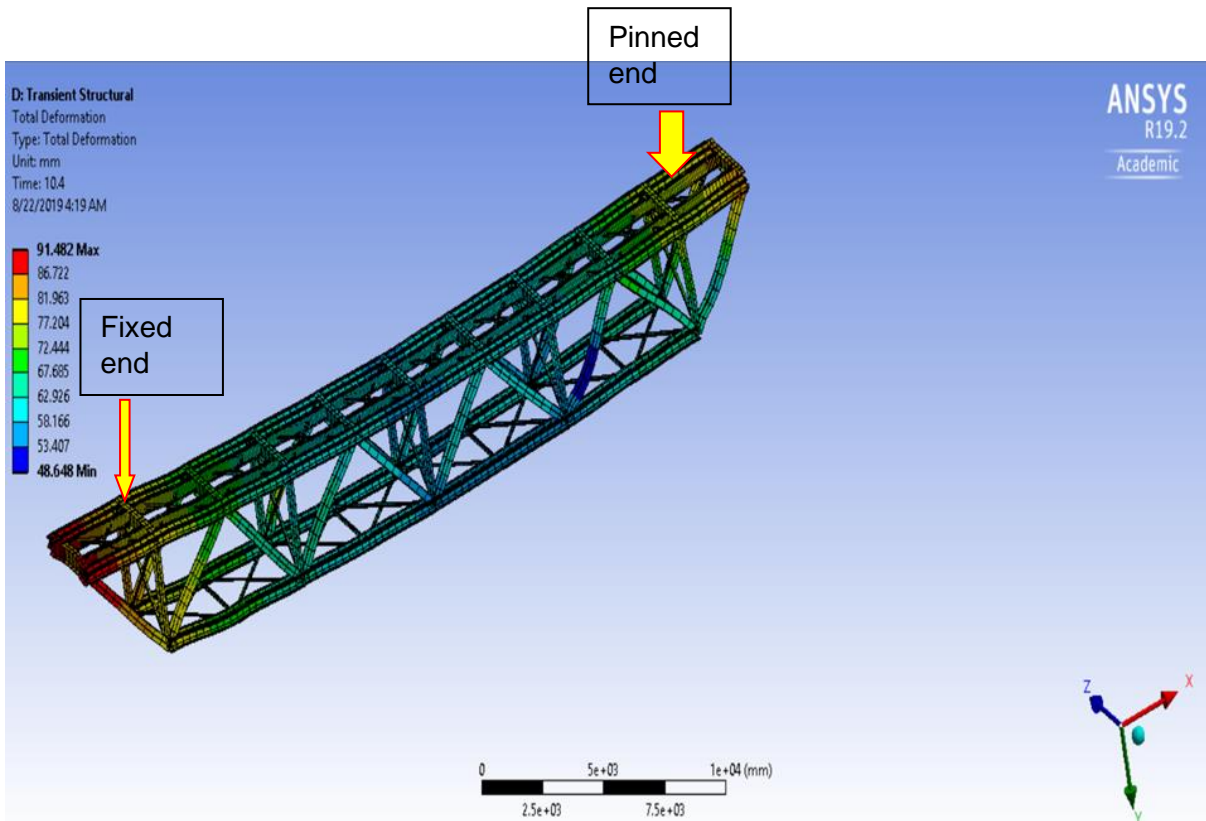
Figure 4.12; Maximum deflection due to the peak ground acceleration at 10.4 seconds
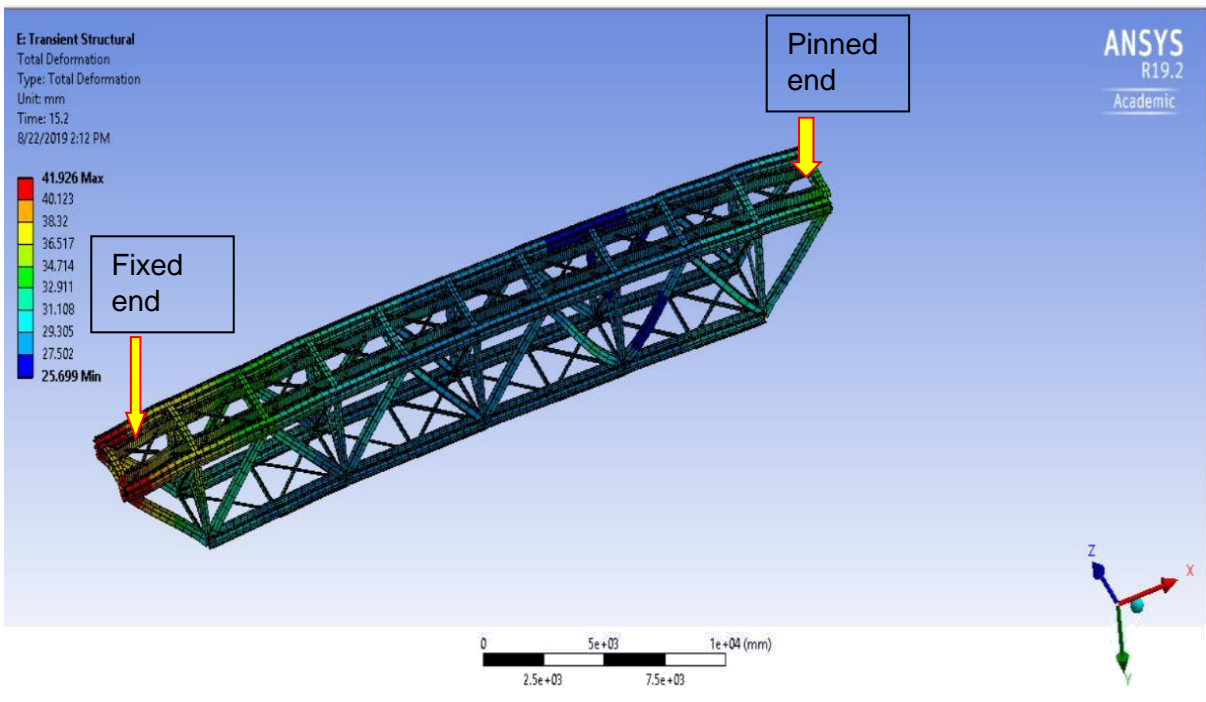
Figure 4.11; Maximum deflection due to peak ground acceleration at 15 seconds.

The animation of the structural behaviour of the bridge superstructure indicates that as the earthquake progresses, the bridge superstructure could slide in the longitudinal direction. This sliding movement will lead to impact between the end-span and the abutment, as well as ponding between adjacent spans in the multi-span Groot Olifants

river bridge. The sliding impact between the bridge superstructure and substructure will potentially result in the shear failure of the bridge bearings (Nielson & DesRoches 2006, Pan et al., 2010), bridge girders as well as the failure of abutment backwalls (DesRoches et al., 2004; Saadeghvaziri & Yazdani-Motlagh 2008). The movement of the bridge superstructure (as observed from the FEA animation) can potentially cause the failure of the bridge bracing system which would significantly reduce the stability in the bridge. The bridge could also move in the transverse direction. This would result in the bridge bearing at the support being overstressed and eventually failing. The results indicate that the structure experiences maximum deflections corresponding to each point where the ground motion acceleration reaches maximum value. After the peak ground acceleration, the deformation of the structure is reduced. As the ground motion acceleration reduces towards the end of the seismic event (39.4 seconds), the bridge superstructure ceases to oscillate, and the deformation experienced by the bridge becomes zero.

From the investigation, it was further noted that for a given ground acceleration, the deformation response of the bridge superstructure is dependent on the natural period of vibration and damping ratio.

4.5 Examination of the results in relation to existing research.

The findings revealed that although the Groot Olifants river bridge was not designed for seismic excitation, the bridge superstructure satisfies the basic seismic load design requirements stipulated in the bridge code. According to researchers such as Haggstrom (2014) and Saadeghvaziri & Yazdani (2008), most large bridges were overdesigned with substantial margins of safety built in to compensate for unknown forces that could affect their integrity over time. Old design codes were very conservative and resulted in overdesigned structured which increases the stability of the old bridge structures. Several parameters such as the earthquake category, soil type and design spectrum play a role in the structural response of bridge structures to seismic excitation. The same conclusion was reached from experimental research carried out on bridges as illustrated Solms (2014) and Haggstrom (2016).

When the bridge superstructure is subjected to ground acceleration (seismic loads) the superstructure oscillates in the direction of the load application. The oscillation results in the lateral, longitudinal and transvers movement of the bridge superstructure. The sliding movement of the bridge superstructure results in pounding of adjacent bridge spans as well as the impact between the bridge superstructure and substructure. This is the primary failure mechanism in bridge superstructure subjected to seismic loads. This was

also noted by Saadeghvaziri & Yazdani-Motlagh (2008), Nielson & DesRoches (2006) as well as Pan et al. (2010).

The failure load of the bridge was predicted to be significantly higher than the ultimate design load. This is attributed to the large factor of safety that was used in the design of the bridge (refer to BS 5400-2 for each type and combination of loading). However, it is not possible to accurately predict the actual load carrying capacity of the bridge using non-destructive load tests. The difficulty in the accurate prediction of the load carrying capacity and remaining life of the steel bridge structure arises due to the difficulty in modelling factors such as corrosion, complex rivet connections as well as accurately determining the actual material properties used on site. The same conclusions were reached by Haggstrom (2016) when testing the Aby bridge to failure.

The critical point to load the Groot Olifants steel truss bridge in order to induce bending failure is at a midspan while the critical point for shear failure is at the support. This occurs because when loaded at midspan, maximum bending occurs and when loaded at the support, the bridge experiences maximum shear. Maximum deflection occurs when maximum loads are applied at midspan. Moreover, the Groot Olifants river bridge displays a bending failure mechanism when the applied load significantly exceeds the design load

The overall findings of the numerical investigation of the structural behaviour of the Groot Olifants river bridge carried out in this investigation are consistent with the findings presented by other scholars such as Solms (2014), Saadeghvaziri & Yazdani-Motlagh (2008), Nielson & DesRoches (2006) as well as Pan et al. (2010). Moreover, the numerical results presented regarding the feasibility of increasing the applied load on the Groot Olifants river bridge are found to be concurrent with the experimental results obtained from case study of the full-scale failure experimental test to collapse carried out on the Åby bridge by Haggstrom (2016).

CHAPTER 5

5.1 Conclusion

The end span from the three spans of the Groot Olifants River bridge located in the Mpumalanga province was modelled and analysed to study the structural behaviour of the bridge when subjected to seismic loads, as well as the feasibility of increasing the applied axle load on the bridge to accommodate the new 44D locomotives in accordance with the requirements set out by the South African freight railway owner. The study revealed that although the Groot Olifants river bridge was not designed for seismic loads, it adheres to the structural requirements as set out in the bridge code and TMH7 clause 3.10.2 for the assessment of bridges using the static method of analysis as discussed in chapter two of this dissertation. The reason for the good structural response when the Groot Olifants river bridge superstructure is subjected to the design response spectrum is not necessarily as a result of good seismic code specifications in the old design code used for the design of this bridge, but rather an indirect effect resulting from the simplicity of the design and the use of large factors of safety as recommended in the old design code. The Groot Olifants river bridge is, however, susceptible to seismic events with a high excitation acceleration such as that of the 0.29 Irpinia earthquake. For the Irpinia earthquake ground motion acceleration (0.29), the Groot Olifants river bridge responds well to the excitation in the Z direction but oscillates excessively due to the excitation in the X and Y directions. This has a large potential of causing the bridge to become unstable, leading to failure. When subject to a high ground acceleration from an earthquake, the maximum tensile strength in some of the critical members are exceeded by as much as 40%. This suggests a high probability of failure. From the transient structural analysis, it is concluded that the Groot Olifants river bridge is not capable of resisting seismic loads from large intensity earthquakes with magnitudes between 6.0 - 6.87 as predicted by Visser & Kijko (2010).

Favourable features of the Groot Olifants river bridge superstructure such as very stiff, lightweight and medium span solution of the truss bridge ensures that the bridge is very effective in carrying increased vertical axle loads. From the numerical evaluations considered in this investigation in conjunction with the case study data from the Åby bridge experimental tests, it is concluded that old steel bridges are capable of resisting significantly larger axle loads. In the case of the Groot Olifants river bridge, it is concluded that the bridge is capable of resisting the 26 tons/ axle loads that will be applied by the new 44D locomotives.

The advancement in technology and the effective numerical methods has allowed for the numerical computation of the structural response of complex structures, producing more accurate results as proven by this investigation. These powerful methods of analysis are capable of determining the complete structural response, "from the elastic range, through cracking and crushing, up to failure" (Zhang, 2015).

Moreover, it has been proven that the methods (FEM) of analysis presently used in THM7 are conservative and require intensive computational efforts. The use of finite element analysis requires the input of several material parameters, which cannot be easily obtained. "At present, finite element analysis is usually considered too impractical for use in civil structural engineering by civil engineering consultants as it often requires input parameters that cannot easily be determined" (Ford, Augarde, & Tuxford, 2003). Similarly, field test observations indicated that the Groot Olifants river bridge is over-designed.

5.2 Recommendations

In this investigation, it was concluded that the Groot Olifants River Bridge meets the basic requirements for seismic loads as set out in TMH7. However, the analysis of the Groot Olifants river bridge does indicate a potential cause for concern when the bridge is subjected to high acceleration ground motion. It is recommended that other bridges on the rail network also be evaluated. Consideration should also be given to evaluating the rivet connections and to take into consideration the impact of rusting of the steel members. The possible risk of damage to the bridge when subjected to high intensity seismic loads indicates a need for solutions to the problem. In conducting further research, a feasibility study must be conducted to determine the most suitable and cost-effective solution. In future research, rails and the sleepers should also be incorporated in the model. In carrying out future work, the substructure/supports/abutments and foundation should be incorporated in the model.

Further extension of this study which includes the degradation effect on seismic behaviour of steel bridges is the future challenge, which is currently followed by the author.

References

Aguilar, R., Montesinos, M., & Ucedas, S. (2017). Analysis of bricks and mortar from Huaca de la Luna in Peru - case study in constructtion materials. *Mechanical characterization of the structural components of pre-Columbiam earthen monuments*, 16-28.

Aktas, Y. D., & Turer, A. (2015). Seismic evaluation and strengthening of nemrut monuments.

Journal of Cultural Heritage, 16, 381-385.

Banerjee, s., & Ganesh, P. s. (2013). Siesmic risk assessment of reinforced concerete bridges in flood prone regions. *Structures and Infrastructure Engineering, 9*, 952-968.

Bayraktar, A., Altunisk, A. C., Sevim, B., & Turker, T. (2007). Modal testing and finite element model calibration of an arch type steel footbridge. *Steel and composite Structures, 7*, 487-502.

Berkley, P. (2018). *PEER Strong Ground Motion Database [Online].* Available:

https://peer.berkeley.edu/peer-strong-ground-motion-database [Accessed 05 September 2019].

Betti, M., & Vignoli, A. (2008). Assessment of seismic resistance of a basilica-type church under earthquake loading: Modelling and analysis. *Advances in Engineering Software, 39*, 258-283.

Brandt, M. (2011). *Seismic Hazard in South Africa.* Western Cape: Council for Geoscience.

Brant, m., & Saunders, I. (2002). Frequency - magnitude relationship and estimated max from micro-seismic data and regional and historical data sets for Southern parts of South Africa. *Africa Geoscience Review, 9(3)*, 199-210.

Bruno, A., Filipe Magalhães, Á., & Joaquim, F. (2014). Modal Analysis for the Rehabilitation Assessment of the Luiz I Bridge. *American Society of civil Enginners*.

Bussata, F., & Moyo, P. (2015). Structural health monitoring of the Olifants river bridge viaduct.

Proc International Heavy Haul Railway Conference. Perth Austraila: IHHA2015.

Chopra, K. A. (2017). *Dynamics of structures, theory and application to earthquake engineering.* Pearson education.

Davies, N., & Kijko, A. (2003). Seismic risk assessment: with an application to the South African insurance industry. *South African Actuarial Journa, 3*, 1–28.

DesRoches, R., Choi, E., Leon, R., Dyke, s., & Massalas, C. (2004). Seismic response of multiple span steel bridges in central and southeastern United States. I: As built. *J. Bridge Eng, 1*.

Drosopoulos, G., Stavroulakis, G., & Massalas, C. (2006). Limit analysis of a single span masonry bridge with unilateral frictional contact interfaces. *Eng. Struct, 28(13)*, 1864–1873.

Ermopoulos, J., & Constantine, C. (2005). Validated analysis and strengthening of a 19th century railway bridge. *Engineering Structures, 28*, 783–792.

Ford, T., Augarde, C., & Tuxford, S. (2003). Modelling masonry arch bridges using commercial finite element software. *School of Engineering, 9th International Conference on Civil and Structural Engineering Computing.* Durham UK: University of Durham.

Haas, T., & Klof, t. v. (2014). Seismic Analysis of URM buildings in South Africa. *South African Insitituate of Civil Engineers*.

Häggström, J. (2016). *Evaluation of the Load Carrying Capacityof a Steel Truss Railway BridgeTesting, Theory and Evaluation.* Phd Theisi: Lulea university of technology.

Hashimoto, k., & Chouw, N. (2003). Investigation of the effect of Kobe earthquake on a three-dimensional soil–structure system. *J. Earthquake Eng, 27*, 1-8.

Hickey, L., Carin, R. W., Cousi, T., Sotelino, E., Easterling, S. P., & Yanev, I. (2010). *It Is Not too Late: Preparing for Asia's Next Big Eathquake With Emphasis on the Philippines,Indonesia and China.*

Hwang, H., Jernigan, J. B., & Lin, Y. W. (2000). Evaluation of seismic damage to Memphis bridges and highway systems. *J. Bridge Eng, 4(322)*, 322–330.

Kijko, A., Durrheim , R., & Mayshree, S. (2009). Seismotectonic models for South Africa: synthesis of geoscientific information, problems, and the way forward. *In: Seismological research letters, 80(1)*, 71-80.

Kim, S., Holub, C., & Elnashai, A. (2011). Analytical assessment of the effect of vertical earthquake motion on RC bridge piers. *J. Struct. Eng*, 252–260.

Kim, Y. R., & Wen, H. (2002). Fracture energy from indirect tension testing. *Asphalt Paving Technol, 71*, 779–793.

Kunnath, S., Erduran, E., Chai, Y., & Yashinsky, M. (2008). Effect of near-fault vertical ground motions on seismic response of highway overcrossings. *J. Bridge Eng, 3(282)*, 282–290.

Kuys, W. (2009). Ore Line Capacity Expansion: Conceptual Design of the Railway line to Increase Capacity. Proc. 9th IHHA Conference. Shanghai, China: (pp. 941-949.).

Marefat, M., Yazdani, M., & Jafari, M. (2017). Seismic assessment of small to medium spans plain concrete arch bridges. *European Journal of Environmental and Civil Engineering*.

Molefe, P. (2018). Transnet Annual Financial Statement. 2019/2020 Transnet Corporate plan.

Motsa, S. (2018). *investigation of the structural behaviour of Megalithic Mnajdra Monument.*

Master's Thesis. Durban: University of Kwazulu Natal.

Nielson, B. G., & DesRoches, R. (2006). Influence of modelling assumptions on the seismic response of multi - span simply suported steel girder bridges in moderate seismic zones. *Engineering Structures, 28(8)*, 1083-1092.

Page, J. (1993). *Masonry Arch Bridges.* Transport Reserch Laboratory.

Pan, Y., Agrawal, A. K., Ghosn, M., & Alampalli, S. (2010). Seismic fragility of multispan simply supported steel highway bridges in New York State. II: Fragility analysis, fragility curves, and fragility surfaces. *J. Bridge Eng*, 462-472.

Priestley, M. N., Verma, R., & Xiao, Y. (1994). Seismic shear strength of reinforced concrete columns. *J. Struct. Eng, 8(2310)*, 2310–2329.

Rao. (2004). *Mechanical Vibrations* (4th ed.).

Saadeghvaziri, A. M., & Yazdani-Motlagh, A. R. (2008). Seismic behavior and capacity/demand analyses of three multi-span simply supported bridges. *Eng. Struct, 30(1)*, 54–66.

Sanchez-Aparico, L. J., Riverio, B., Gonzalaz-Aguilera, D., & Ramos, L. F. (2014). The combination of Geomatric approaches and operational modal analysis to improve calibration of finite element models: A case study in Saint Torcato Church (Guimaraes, Portugal). *Construction and Building Materials, 70*, 118-129.

SATS (1983). *Bridge code.* Pretoria: Department of Transport

Soetardjo, M. U., Arnold, E. P., Soetadi, S. I., & Kertapati, E. K. (1985). Series on Seismology.

Indonesia: Southeast Asia Association of Seismology and Earthquake, 5.

Solms, M. (2016). Siesmic evaluation of the northbound N1/R300 bridge interchange. *Journal of South Africa Institute of Civil Engineering, 58*, 62-71.

Sudarsanan, N., Arulrajah, A., Karpurapu, R., & Amrithalingam, V. (2019). Digital Image Correlation Technique for Measurement of Surface Strains in Reinforced Asphalt Concrete Beams under Fatigue Loading. *Journal of Materials in Civil Engineering, 31(8)*.

Sun, Z., Wand, D., Guo, X., Si, B., & Huo, Y. (2012). Lessons learned from the damaged Huilan interchange in the 2008 Wenchuan earthquake. *J. Bridge Eng*, 15–24.

Sutton, M. A., Wolters, W. J., Ranson, W. F., McNeill, R. S., & Peters, W. H. (1983). Determination of displacements using an improveddigital correlation method. *Image Vis. Comput, 1(3)*, 133-139.

Taliercio, A., & Binda, L. (2007). The Basilica of San Vitale in Ravenna: Investigation on the current structural faults and their mid-term evolution. *Journal of Cultural Heritage, 8*, 99-118.

Terzi, V. G., & Ignatakis, C. E. (2018). Nonlinear finite element analyses for the restoration study of Xana, Greece. *Engineering Structures*, 96-107.

Tian, L., Pan, B., Cai, Y., Liang, H., & Zhao, Y. (2013). Application of digital image correlation for long-distance bridge deflection measurement. *International Conference on Optics in Precision Engineering and Nanotechnology.*

TMH7. (1981). *Part 1-3 Code of Practice for the Design of Highway Bridges and Culverts in South Africa.* Pretoria: Department of Transport.

Toshiro, H., Yoshitaka, M., & Takakichi, k. (2000). *Nonlinear dynamic behavior and seismic isolation of steel towers of cable stayed bridges under earthquake ground motion.* 12wcee.

Trevor, N. H., & Van der Kolf, T. (2014). Seismic Analysis of URM Buildings in S. Africa, World Academy of Science, Engineering and Technology. *International Journal of Civil and Environmental Engineering, 8(12)*.

Yashinsky, M. (1998). The Loma Prieta, California, Earthquake of October 17, 1989—Highway System.

Veldsman, A., & Mulde, M. (2005). Progress on the roll-out of ECPB/WDP systems on Spoornet.

Experiences gained on the Coal Line and Ore-Line. *Proc. 8th IHHA Conference.*, (pp.

699-709.). Rio de Janeiro, Brazil:

Vercher, J., Gil, E., Mas, A., & Lerma, C. (2015). Diagnosis and Intervention Criteria in Slabs Damaged by Severe Corrosion of Prestressed Joists. *Journal of Performance of Constructed Facilities, 29.*

Vestroni, F., Beolchini, G., & Antonacci, E. (1996). Identification of dynamic characteristics of masonry buildings from forced vibration tests. *Proceedings of the 11th world conference on earthquake engineering.*

Visser, P., & Kijko, A. (2010). *South Africa Spotlight on Earthquake.* Johannesburg: AON Benfield.

Von Gericke, R. E. (1986). Measures taken by the South African Transport Services to Reduce Transportation Costs of Coal on the Ermelo - Richards Bay Line. *Proc. 3rd International Heavy Haul Railway Conference.* (pp. 396-412.). Vancouver, Canada: IHHA.

Wang, Z., Due nas Osorio, L., & Padgett, J. E. (2013). Seismic response of a bridge-soil-foundation system under the combined effect of vertical and horizontal ground motions. *Earthquake Eng. Struct. Dyn, 42*(4), 545–564.

Wei-Xin, R. A. (2004). Experimental and Analytical Modal Analysis of Steel Arch Bridge. *Journal of structural Engineering ASCE.*

Wium, J. A. (2010). Background to Draft SANS 10160 (2009): Part 4 Seismic Loading. *Journal of the South African Institution of Civil Engineering.*

Wu, G., Shi, W., Chen, Z., Fu, J., Gup, N., & Hou, S. (2011). Finite element modal analysis and test modal analysis of the control cab. *Proceedings of 2011 International Conference on Electronic & Mechanical Engineering and Information Technology.*

Yanev, P. A., Yanev, P. I., & Medina, F. (2010). *The magnitude 808 offshore maule region Chile eathquake of February 27.* Chile: Wolrd Bank.

Yang, J., & Lee, C. (2007). Characteristics of vertical and horizontal ground motions recorded during the Niigata-ken Chuetsu, Japan Earthquake of 23 October 2004. *Engineering Geology, 94(1)*, 50-64.

Yoneyama, S., Kitagawa, A., Iwata, S., Tani, K., & Kikuta, H. (2007). Bridge deflection measurement using Digital Image Corrolation . *Experimental techniques*, 34-40.

Yue, Q. Z., & Morin, I. (1996). Digital image processing for aggregateorientation in asphalt concrete mixtures. *Can. J. Civ. Eng, 23 (2)*, 480–489.

Zhang, Y. (2015). *Advanced Nonlinear Analysis of Masonry Arch Bridges. PhD Eng. Thesis, Department of Civil and Environmental Engineering.* London: Imperial College.

Živanović, S., Pavic, A., & Reynolds, P. (2006). Modal testing and Fe model tuning of a lively footbridge structure. *Engineering structures, 28*, 587-86.

Appendix A: 44D Boogie arrangement

Appendix B (44D locomotive)
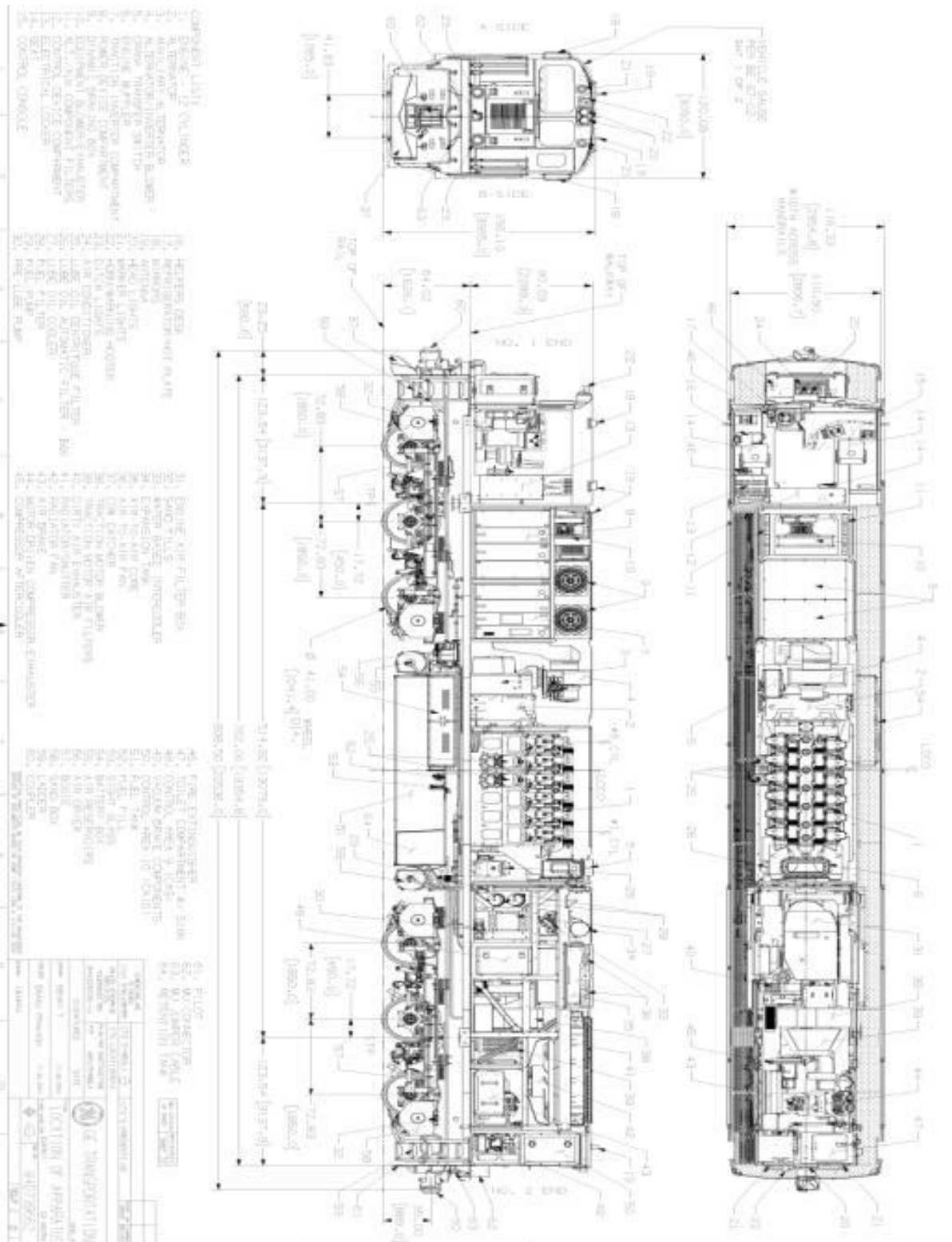
Appendix C (FY locomotive)

Appendix D boogie arrangement

Appendix E (Groot Olifants River Bridge)

Appendix F (Original drawings of the Groot Olifants River Bridge)

COLONIAL Nº 68669

C S A R — 30 M CLEAR DECK SPAN —
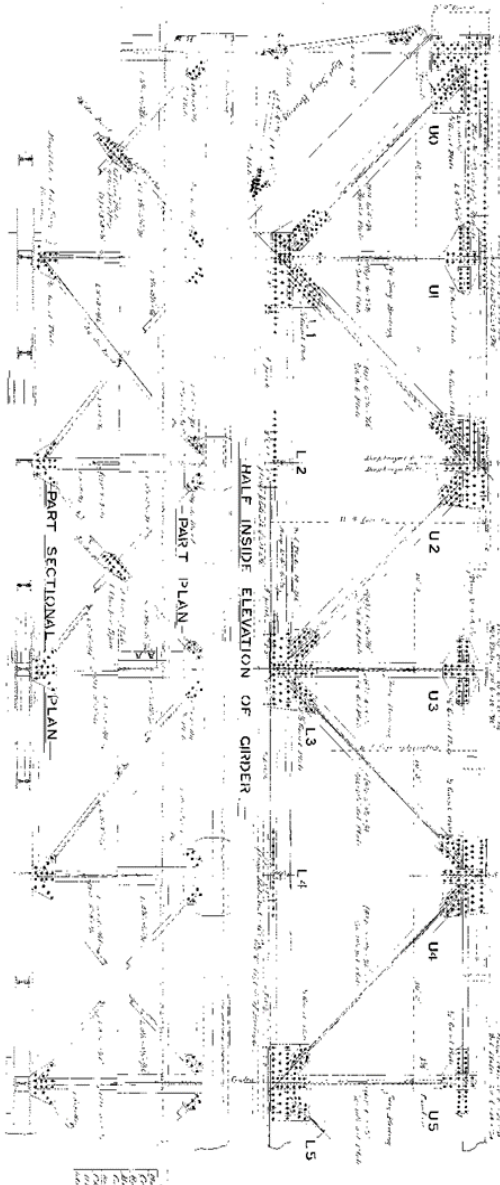
REQUISITION Nº 943

SCALE ½ = 1 · 6 TO ONE FOOT

— HALF INSIDE ELEVATION OF GIRDER —

U0 U1 U2 U3 U4 U5

L2 L3 L4 L5

— HALF SECTION A.A —

— HALF SECTION B.B —

L3

U3

U0

— PART SECTIONAL PLAN —

— PART PLAN —

— DETAIL OF CHEQUERED PLATE —

— SLEEPER BOLT —

— RAILBEARER & BRACKET —

— DRAWING Nº 60 A —

BE 7498.
DRAWER 508.

BE 7498   508

Appendix G (Original drawings of the Åby River Bridge)
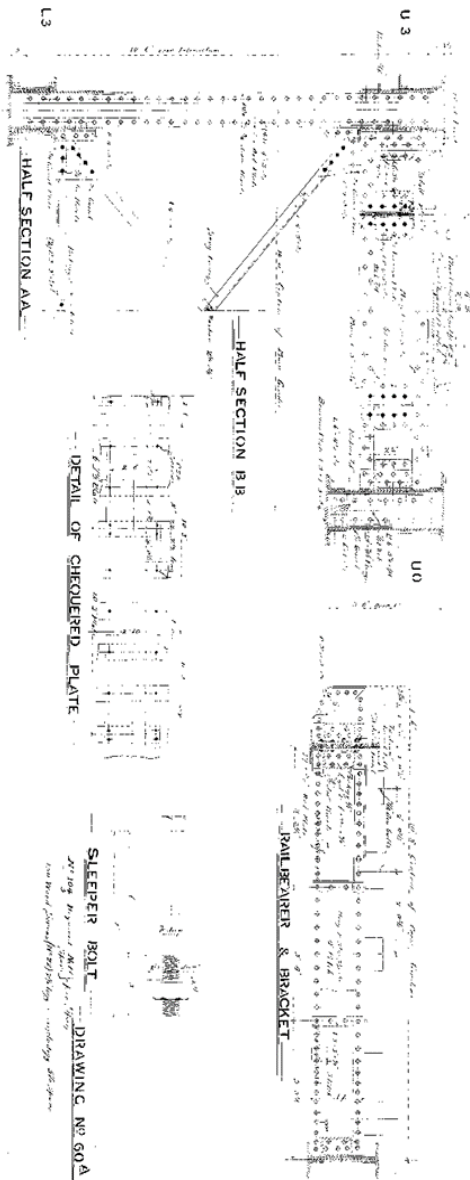
Appendix H (Truss bridge components)